stage 4S infants who receive no (or minimal) treatment based on the lack of MNA, even though current statistics show that 1 in 10 of these infants will eventually die of NB. In this paper, we propose that determination of low netrin-1 level confirms a good prognosis for these infants without therapy, whereas the infants with high netrin-1 expression should be considered for more intensive treatment. Regarding infants or children with high netrin-1–expressing NB tumors, an alternative or supplementary targeted treatment based on disruption of the netrin-1 autocrine survival loop may improve standard high-dose chemotherapy regimen efficiency. We propose that a treatment based on inhibition of the interaction between netrin-1 and its dependence receptors, or inhibition of the ability of netrin-1 to multimerize its receptors, could potentially improve the survival of a large fraction of the patients suffering from aggressive NB. Moreover, it is interesting to note that no correlation between netrin-1 up-regulation and molecular signature of apoptosis and invasion was observed in NB tumors (Fig. S1 D), strengthening the case for netrin-1 as an original target for NB. Future preclinical and clinical studies should assess whether such therapeutic strategies, which could include small molecules (drugs), monoclonal antibodies, or the DCC-5Fbn recombinant protein presented in this paper, used alone or in combination with standard chemotherapy, could be of therapeutic benefit for infants and children with NB.

MATERIALS AND METHODS

Cell lines, transfection procedure, and reagents. Human NB cell lines were obtained from the tumor banks at Centre Léon Bérard and at Institut Gustave Roussy. More specifically, IMR32 and CLB-Ge2 cell lines were cultured in RPMI 1640 GlutaMAX medium (Invitrogen) containing 10% FBS. IGR-N-91 cell line and its derivatives, as well as HEK293T cells, were cultured in DME medium (Invitrogen) containing 10% FBS. Cell lines were transfected using Lipofectamine 2000 reagent (Invitrogen) for siRNA or Lipofectamine Plus reagent (Invitrogen) for plasmids. Netrin-1 was obtained from Axxora and was used at a concentration of 150 ng/ml in all in vitro assays.

Human NB tumor samples and biological annotations. According to parental consent, surgical human NB tumor material was immediately frozen. Material and annotations were obtained from the Biological Resources Centers of both national referent Institutions for NB treatment (Centre Léon Bérard and at Institut Gustave Roussy). Protocols using human material were approved by the local ethics Committees of Lyon University and Paris XI University. MYCN genomic content was assessed on histologically qualified tumors as previously described (52). For immunohistochemistries, 5-µm sections were prepared and frozen at −80°C.

Plasmid constructs, siRNA, and DCC-5Fbn production. The dominant-negative mutant for UNC5H and DCC (pCR-UNC5H2-IC-D412N and pCR-DCC-IC-D1290N, respectively) and the plasmids encoding Neogenin (pCDNA3-Neogenin) and UNC5H1 (pCDNA3.1-UNC5H1-HA) have been previously described (1, 2, 5). The plasmids encoding UNC5H2 (pCDNA3.1-UNC5B-HA), UNC5H3 (pCDNA3-UNC5C-HA), and UNC5H4 (pCAG3-hU5H4-His) were gifts from H. Arakawa (National Cancer Institute, Tokyo, Japan), M. Tessier-Lavigne (Genentech, San Francisco, CA), K.L. Guan (University of Michigan, Ann Arbor, MI), and N. Yamamoto (Osaka University, Osaka, Japan). Human netrin-1–encoding plasmid (peak8-hNTN1-His) was obtained from D.E. Bredesen (The Buck Institute for Age Research, Novato, CA). Ps974-DCC-5Fbn allowing bacterial expression of the fifth fibronectin type III domain of DCC was obtained by inserting a PstI–BamH1 DNA fragment generated by PCR using pDCC-CMV-S as a template. DCC-5Fbn production was performed using a standard procedure. In brief, BL21 cells were forced to express DCC-5Fbn in response to imidazole, and the BL21 lysate was subjected to affinity chromatography using FLAG-Sepharose (Sigma-Aldrich). A peptide corresponding to the ectodomain of IL3R was produced in the same conditions and used as a control. For cell culture use, netrin-1, DCC, and neogenin siRNAs (Santa Cruz Biotechnology, Inc.) were designed as a pool of three target-specific 20–25-nt siRNAs. UNC5H1, UNC5H2, UNCH3, and UNC5H4 siRNAs were designed by Sigma-Aldrich. MYCN siRNA was designed by Thermo Fisher Scientific.

Cell death assays. 2×10^5 cells were grown in serum-poor medium and were treated (or not) with 1 µg/ml DCC-5Fbn or transfected with siRNA using Lipofectamine 2000. Cell death was analyzed using trypan blue staining procedures as previously described (1). The extent of cell death is presented as the percentage of trypan blue–positive cells in the different cell populations. Apoptosis was monitored by measuring caspase-3 activity as described previously (1) using the Caspase 3/CPP32 Fluorimetric Assay kit (Gentaur). For detection of DNA fragmentation, treated cells were cytospun, and TUNEL was performed with 300 U/ml TUNEL enzyme and 6 µM biotinylated dUTP (Roche) as previously described (53).

Q-RT-PCR. To assay netrin-1, DCC, and UNC5H receptor expression in NB samples, total RNA was extracted from histologically qualified tumor biopsies (>60% immature neuroblasts) using the NucleoSpin RNAII kit (Macherey-Nagel), and 200 ng were reverse transcribed using 1U Superscript II reverse transcription (Invitrogen), 1U RNase inhibitor (Roche), and 250 ng of random hexamer (Roche). Total RNA was extracted from mouse and human cell lines using the NucleoSpin RNAII kit and 1 µg was reverse transcribed using the iScript cDNA Synthesis kit (Bio-Rad Laboratories). Real-time Q-RT-PCR was performed on a LightCycler 2.0 apparatus (Roche) using the LightCycler FastStart DNA Master SYBER Green I kit (Roche). Reaction conditions for all optimal amplifications, as well as primer selection for murine and human netrin-1, DCC, and UNC5H1-4, were determined as already described. The ubiquitously expressed human HPRT genes showing the least variability in expression in NB was used as an internal control (54). The sequences of the primers are the following: NTN1, 5′-TGCAAGAAGGACTATGCCGTC-3′ and 5′-GCTCGTGCCCTGCTTATACAC-3′; UNC5H1, 5′-CATCACCAAGGACACAAGGTTTGC-3′ and 5′-GGCTGGAAATTATCTTCTGCCGAA-3′; UNC5H2, 5′-GGGCTGGAGGATTACTGGTG-3′ and 5′-TGCAGGAGAACCTCATGGTC-3′; UNC5H3, 5′-GCAAATTGCTGGCTAAATATCAGGAA-3′ and 5′-GCTCCACTGTGTTCAGGCTAAATCTT-3′; UNC5H4, 5′-GGTGAACCCAGCCTCCAGTCAG-3′ and 5′-CTTCCACTGACATCACTTCCTCCC-3′; DCC, 5′-AGCCAATGGGAAAATTACTGCTTAC-3′ and 5′-AGGTTGAGATCCATGATTTGATGAG-3′; and HPRT, 5′-TGACACTGGCAAAACAATGCA-3′ and 5′-GGTCCTTTTCACCAGCAAGCT-3′.

Genomic DNA quantification. Genomic DNA from IMR32 and CLB-Ge2 cells was extracted with the NucleoSpin Tissue kit (Macherey-Nagel). 50 ng of genomic DNA was used to perform quantitative PCR using primers specific to *NTN1* and *MYCN* genomic sequences. Real-time quantitative PCR was performed on a LightCycler 2.0 apparatus using the Light Cycler FastStart DNA Master SYBER Green I kit. *NAGK* (the *N*-acetylglucosamine kinase gene), which is located on chromosome 2 similarly to the *MYCN* gene but separated from the MYCN amplicon, was used as an internal control gene to determine the gene dosage (55). For each pair of primers, genomic DNA amplification was assessed by polymerase activation at 95°C for 10 min, followed by 35 cycles at 95°C for 10 s, 65°C for 30 s, and 72°C for 10 s. The sequences of the primers are the following: *NTN1*, 5′-CTGTGTCCCCCACTTGTTCT-3′ and 5′-CCATGAACCCCACTGACTCT-3′; *MYCN*, 5′-GTGCTCTCCAATTCTCGCCT-3′ and 5′-GATGGCCTAGAGGAGGGCT-3′; and *NAGK*, 5′-TGGGCAGACACATCGTAGCA-3′ and 5′-CACCTTCACTCCCACCTCAAC-3′.

Immunohistochemistry and immunoblotting analysis. 10^5 cells were centrifugated on coverslips with a cytospinner (Shandon Cytospin 3; Thermo Fisher Scientific). Tumor slides and cells were fixed in 4% paraformaldehyde. The slides were then incubated at room temperature for 1 h with an antibody recognizing the human netrin-1 (1:150; R&D Systems), UNC5H1 (1:100; Abcam), UNC5H3 (1:100; R&D system), or UNC5H4 (1:100; Santa Cruz Biotechnology, Inc.). After rinsing in PBS, the slides were incubated with an Alexa 488 donkey anti–rat antibody (Invitrogen), an Alexa 488 donkey anti–rabbit antibody (Invitrogen), a Cy3 donkey anti–mouse antibody (Jackson ImmunoResearch Laboratories), or an Alexa 488 donkey anti–goat antibody (Invitrogen), respectively. For tumor slides, netrin-1 and UNC5H4 signals were amplified using biotinyl-tyramide (TSA; Thermo Fisher Scientific) and Alexa 488–streptavidin (Invitrogen). Nuclei were visualized with Hoechst staining. Densitometric value corresponding to netrin-1 signal was quantified with AxioVision Release 4.6 software. Immunoblots were performed as already described using anti–phospho-DAPK and anti-DAPK (Sigma-Aldrich) (38), anti-DCC (1:500; Santa Cruz Biotechnology, Inc.), anti-neogenin (1:500; Santa Cruz Biotechnology, Inc.), anti-HA (1:7,500; Sigma-Aldrich), anti-HIS (1:1,000; QIAGEN), anti-MYCN (1:1000; BD), or anti-β-actin (1:1,000; Millipore) antibodies.

Netrin-1 ELISA assay. Detection of netrin-1 protein in IMR32 and CLB-Ge2 cell culture medium was performed using a modified ELISA assay. In brief, 96-well plates (Nunc-Immuno plate MaxiSorp; Thermo Fisher Scientific) were coated with 200 ng/well of purified recombinant extracellular domain of DCC (DCC-Ec-Fc). To minimize aspecific binding, each well was incubated with 100 µl of blocking solution, containing 5% (wt/vol) BSA (Sigma-Aldrich) in 0.05% PBS-Tween. 3 ml FBS free cell culture medium was added sequentially (300 µl/well) to coated 96-well plates and incubated for 1 h at 37°C. After three washes with 0.5% BSA/PBS, 100 µl of rat anti–netrin-1 antibody (diluted 1:500 in blocking solution) was added to each well and incubated for 30 min at 37°C. After extensive washing, each well was incubated with 100 µl HRP-conjugated goat anti–rat antibody (1:1,000; Jackson ImmunoResearch Laboratories) for 30 min at 37°C. After removal of unbound antibody by three washes in 0.5% BSA/PBS, the plates were incubated for 5 min at room temperature with ECL Western Blotting Substrate (Thermo Fisher Scientific). Luminescent signal was measured using a Luminoskan Ascent apparatus (Thermo Fisher Scientific).

Reporter assay. 10^5 cells were plated in 12-well plates and transfected with the firefly luciferase reporter under the control of the netrin-1 promoter (pGL3-NetP-Luc) or the pGL3 empty vector. All transfections were done in triplicate and the Dual-Luciferase Reporter Assay system (Promega) was performed 48 h after transfection according to the manufacturer's protocol, using the Luminoskan Ascent apparatus. As an internal control of transfection efficiency, the renilla luciferase-encoding plasmid (pRL-CMV; Promega) was cotransfected, and for each sample firefly luciferase activity was normalized to the renilla luciferase activity.

Chicken model for NB progression and dissemination. 10^7 NB cells suspended in 40 µl of complete medium were seeded on 10-d-old chick CAM. 10 µg DCC-5Fbn or the same PBS volume was injected in the tumor on days 11 and 14. For siRNA treatment, 4 µg of scramble or netrin-1 siRNA was injected under the same conditions as for DCC-5Fbn. On day 17, tumors were resected and the area was measured with AxioVision Release 4.6 software (Carl Zeiss, Inc.). To test the effect of DCC-5Fbn on metastasis regression, 3 µg DCC-5Fbn or PBS was injected on days 14 and 15 in a chorioallantoic vessel. To assess metastasis, lungs were harvested from the tumor-bearing embryos and genomic DNA was extracted with a NucleoSpin Tissue kit (Macherey-Nagel). Metastasis was quantified by PCR-based detection of the human Alu sequence using the primers 5′-ACGCCTGTAATCCCAGCACTT-3′ (sense) and 5′-TCGCCCAGGCTGGAGTGCA-3′ (antisense) with chick GAPDH-specific primers (sense, 5′-GAGGAAAGGTCGCCTGGTGGATCG-3′; antisense, 5′-GGTGAGGACAAGCAGTGAGGAACG-3′) as controls. For both couples of primers, metastasis was assessed by polymerase activation at 95°C for 2 min followed by 30 cycles at 95°C for 30 s, 63°C for 30 s, and 72°C for 30 s. Genomic DNA extracted from lungs of healthy chick embryos was used to determine the threshold between NB cell–invaded and –noninvaded lungs. To monitor apoptosis in primary tumors, primary tumors and surrounding CAM were resected and broken up in lysis buffer and caspase-3 activity was measured using the Caspase 3/CPP32 Fluorimetric Assay kit.

NB metastasis in *nude* mice. 7-wk-old (20–22 g body weight) female athymic nu/nu mice were obtained from Charles River Laboratories. The mice were housed in sterilized filter-topped cages and maintained in a pathogen-free animal facility. IGR-N-91–derived PTX and Myoc cell lines were implanted by i.v. injection of 10^6 cells in 130 µl of PBS into a tail vein (day 0). 20 µg DCC-5Fbn or PBS with equal volume was i.p. injected daily during 22 d. Lungs were harvested on day 23. Lung genomic DNA was extracted with the NucleoSpin Tissue kit, and quantification of human tumor cells in lungs was done by PCR-based detection of the human Alu sequence using the primers 5′-CACCTGTAATCCCAGCACTTT-3′ (sense) and 5′-CCCAGGCTGGAGTGCAGT-3′ (antisense), using 25 ng of genomic DNA as previously described (56). PCR was performed under the following conditions: 95°C for 2 min, 30 cycles at 95°C for 30 s, 65°C for 20 s, and 72°C for 20 s. Quantification of human DNA in mice lungs was based on a standard curve using human genomic DNA isolated from PTX and Myoc cell lines.

Online supplemental material. Fig. S1 associates netrin-1 and DCC expression in NB tumors with their apoptosis and invasion molecular signatures obtained with microarrays. Fig. S2 presents netrin-1 mRNA and protein expression in NB cell lines and shows CLB-VolMo netrin-1–high cell line sensitivity to DCC-5Fbn decoy fragment. In Fig. S3, MYCN and neogenin implication in netrin-1 siRNA–induced cell death is studied, and specificity and efficiency of UNC5H siRNAs are presented at the mRNA, protein, and cellular levels. Online supplemental material is available at http://www.jem.org/cgi/content/full/jem.20082299/DC1.

We thank M.M. Coissieux, C. Guix, M.L. Puiffe, I. Iacono, and S. Bréjon for technical assistance. We thank J. Bouzas, J.G. Delcros, and P. Leissner for excellent support. We thank Dale E. Bredesen for precious advice and text correction.

This work was supported by the Ligue Contre le Cancer (P. Mehlen), the Agence Nationale de la Recherche (P. Mehlen), the Institut National du Cancer (J. Bénard, A. Puisieux, and P. Mehlen), the Société Francaise des Cancers de l'Enfant (J. Bénard), The French Health Minister (J. Bénard and D. Valteau-Couanet), The EU fundings Hermione (P. Mehlen) and APOSYS (P. Mehlen), the Centre National de la Recherche Scientifique, and the Centre Léon Bérard.

The authors have no conflicting financial interests.

Submitted: 14 October 2008
Accepted: 3 March 2009

REFERENCES

1. Mehlen, P., S. Rabizadeh, S.J. Snipas, N. Assa-Munt, G.S. Salvesen, and D.E. Bredesen. 1998. The DCC gene product induces apoptosis by a mechanism requiring receptor proteolysis. *Nature*. 395:801–804.
2. Llambi, F., F. Causeret, E. Bloch-Gallego, and P. Mehlen. 2001. Netrin-1 acts as a survival factor via its receptors UNC5H and DCC. *EMBO J.* 20:2715–2722.
3. Thibert, C., M.A. Teillet, F. Lapointe, L. Mazelin, N.M. Le Douarin, and P. Mehlen. 2003. Inhibition of neuroepithelial patched-induced apoptosis by sonic hedgehog. *Science*. 301:843–846.
4. Stupack, D.G., X.S. Puente, S. Boutsaboualoy, C.M. Storgard, and D.A. Cheresh. 2001. Apoptosis of adherent cells by recruitment of caspase-8 to unligated integrins. *J. Cell Biol.* 155:459–470.
5. Matsunaga, E., S. Tauszig-Delamasure, P.P. Monnier, B.K. Mueller, S.M. Strittmatter, P. Mehlen, and A. Chedotal. 2004. RGM and its receptor neogenin regulate neuronal survival. *Nat. Cell Biol.* 6:749–755.
6. Rabizadeh, S., J. Oh, L.T. Zhong, J. Yang, C.M. Bitler, L.L. Butcher, and D.E. Bredesen. 1993. Induction of apoptosis by the low-affinity NGF receptor. *Science*. 261:345–348.
7. Bordeaux, M.C., C. Forcet, L. Granger, V. Corset, C. Bidaud, M. Billaud, D.E. Bredesen, P. Edery, and P. Mehlen. 2000. The RET

proto-oncogene induces apoptosis: a novel mechanism for Hirschsprung disease. *EMBO J.* 19:4056–4063.
8. Mourali, J., A. Benard, F.C. Lourenco, C. Monnet, C. Greenland, C. Moog-Lutz, C. Racaud-Sultan, D. Gonzalez-Dunia, M. Vigny, P. Mehlen, et al. 2006. Anaplastic lymphoma kinase is a dependence receptor whose proapoptotic functions are activated by caspase cleavage. *Mol. Cell. Biol.* 26:6209–6222.
9. Tauszig-Delamasure, S., L.Y. Yu, J.R. Cabrera, J. Bouzas-Rodriguez, C. Mermet-Bouvier, C. Guix, M.C. Bordeaux, U. Arumae, and P. Mehlen. 2007. The TrkC receptor induces apoptosis when the dependence receptor notion meets the neurotrophin paradigm. *Proc. Natl. Acad. Sci. USA.* 104:13361–13366.
10. Del Rio, G., D.J. Kane, K.D. Ball, and D.E. Bredesen. 2007. A novel motif identified in dependence receptors. *PLoS One.* 2:e463.
11. Mehlen, P., and C. Thibert. 2004. Dependence receptors: between life and death. *Cell. Mol. Life Sci.* 61:1854–1866.
12. Bredesen, D.E., P. Mehlen, and S. Rabizadeh. 2005. Receptors that mediate cellular dependence. *Cell Death Differ.* 12:1031–1043.
13. Serafini, T., S.A. Colamarino, E.D. Leonardo, H. Wang, R. Beddington, W.C. Skarnes, and M. Tessier-Lavigne. 1996. Netrin-1 is required for commissural axon guidance in the developing vertebrate nervous system. *Cell.* 87:1001–1014.
14. Keino-Masu, K., M. Masu, L. Hinck, E.D. Leonardo, S.S. Chan, J.G. Culotti, and M. Tessier-Lavigne. 1996. Deleted in colorectal cancer (DCC) encodes a netrin receptor. *Cell.* 87:175–185.
15. Forcet, C., E. Stein, L. Pays, V. Corset, F. Llambi, M. Tessier-Lavigne, and P. Mehlen. 2002. Netrin-1-mediated axon outgrowth requires deleted in colorectal cancer-dependent MAPK activation. *Nature.* 417:443–447.
16. Ackerman, S.L., L.P. Kozak, S.A. Przyborski, L.A. Rund, B.B. Boyer, and B.B. Knowles. 1997. The mouse rostral cerebellar malformation gene encodes an UNC-5-like protein. *Nature.* 386:838–842.
17. Hong, K., L. Hinck, M. Nishiyama, M.M. Poo, M. Tessier-Lavigne, and E. Stein. 1999. A ligand-gated association between cytoplasmic domains of UNC5 and DCC family receptors converts netrin-induced growth cone attraction to repulsion. *Cell.* 97:927–941.
18. Mehlen, P., and A. Puisieux. 2006. Metastasis: a question of life or death. *Nat. Rev. Cancer.* 6:449–458.
19. Grady, W.M. 2007. Making the case for DCC and UNC5C as tumor-suppressor genes in the colon. *Gastroenterology.* 133:2045–2049.
20. Mazelin, L., A. Bernet, C. Bonod-Bidaud, L. Pays, S. Arnaud, C. Gespach, D.E. Bredesen, J.Y. Scoazec, and P. Mehlen. 2004. Netrin-1 controls colorectal tumorigenesis by regulating apoptosis. *Nature.* 431:80–84.
21. Bernet, A., L. Mazelin, M.M. Coissieux, N. Gadot, S.L. Ackerman, J.Y. Scoazec, and P. Mehlen. 2007. Inactivation of the UNC5C Netrin-1 receptor is associated with tumor progression in colorectal malignancies. *Gastroenterology.* 133:1840–1848.
22. Fearon, E.R., K.R. Cho, J.M. Nigro, S.E. Kern, J.W. Simons, J.M. Ruppert, S.R. Hamilton, A.C. Preisinger, G. Thomas, K.W. Kinzler, et al. 1990. Identification of a chromosome 18q gene that is altered in colorectal cancers. *Science.* 247:49–56.
23. Kinzler, K.W., and B. Vogelstein. 1996. Lessons from hereditary colorectal cancer. *Cell.* 87:159–170.
24. Thiebault, K., L. Mazelin, L. Pays, F. Llambi, M.O. Joly, J.C. Saurin, J.Y. Scoazec, G. Romeo, and P. Mehlen. 2003. The netrin-1 receptors UNC5H are putative tumor suppressors controlling cell death commitment. *Proc. Natl. Acad. Sci. USA.* 100:4173–4178.
25. Shin, S.K., T. Nagasaka, B.H. Jung, N. Matsubara, W.H. Kim, J.M. Carethers, C.R. Boland, and A. Goel. 2007. Epigenetic and genetic alterations in Netrin-1 receptors UNC5C and DCC in human colon cancer. *Gastroenterology.* 133:1849–1857.
26. Evans, A.E., G.J. D'Angio, and J. Randolph. 1971. A proposed staging for children with neuroblastoma. Children's cancer study group A. *Cancer.* 27:374–378.
27. Matthay, K.K., J.G. Villablanca, R.C. Seeger, D.O. Stram, R.E. Harris, N.K. Ramsay, P. Swift, H. Shimada, C.T. Black, G.M. Brodeur, et al. 1999. Treatment of high-risk neuroblastoma with intensive chemotherapy, radiotherapy, autologous bone marrow transplantation, and 13-cis-retinoic acid. Children's Cancer Group. *N. Engl. J. Med.* 341:1165–1173.
28. Valteau-Couanet, D., J. Michon, A. Boneu, C. Rodary, Y. Perel, C. Bergeron, H. Rubie, C. Coze, D. Plantaz, F. Bernard, et al. 2005. Results of induction chemotherapy in children older than 1 year with a stage 4 neuroblastoma treated with the NB 97 French Society of Pediatric Oncology (SFOP) protocol. *J. Clin. Oncol.* 23:532–540.
29. Reale, M.A., M. Reyes-Mugica, W.E. Pierceall, M.C. Rubinstein, L. Hedrick, S.L. Cohn, A. Nakagawara, G.M. Brodeur, and E.R. Fearon. 1996. Loss of DCC expression in neuroblastoma is associated with disease dissemination. *Clin. Cancer Res.* 2:1097–1102.
30. Krause, A., V. Combaret, I. Iacono, B. Lacroix, C. Compagnon, C. Bergeron, S. Valsesia-Wittmann, P. Leissner, B. Mougin, and A. Puisieux. 2005. Genome-wide analysis of gene expression in neuroblastomas detected by mass screening. *Cancer Lett.* 225:111–120.
31. Furne, C., N. Rama, V. Corset, A. Chedotal, and P. Mehlen. 2008. Netrin-1 is a survival factor during commissural neuron navigation. *Proc. Natl. Acad. Sci. USA.* 105:14465–14470.
32. Paradisi, A., C. Maisse, A. Bernet, M. Coissieux, M. Maccarrone, J. Scoazec, and P. Mehlen. 2008. NF-κB regulates netrin-1 expression and affects the conditional tumor suppressive activity of the netrin-1 receptors. *Gastroenterology.* 135:1248–1257.
33. Fitamant, J., C. Guenebeaud, M.M. Coissieux, C. Guix, I. Treilleux, J.Y. Scoazec, T. Bachelot, A. Bernet, and P. Mehlen. 2008. Netrin-1 expression confers a selective advantage for tumor cell survival in metastatic breast cancer. *Proc. Natl. Acad. Sci. USA.* 105:4850–4855.
34. Reale, M.A., G. Hu, A.I. Zafar, R.H. Getzenberg, S.M. Levine, and E.R. Fearon. 1994. Expression and alternative splicing of the deleted in colorectal cancer (DCC) gene in normal and malignant tissues. *Cancer Res.* 54:4493–4501.
35. Meyerhardt, J.A., A.T. Look, S.H. Bigner, and E.R. Fearon. 1997. Identification and characterization of neogenin, a DCC-related gene. *Oncogene.* 14:1129–1136.
36. Cole, S.J., D. Bradford, and H.M. Cooper. 2007. Neogenin: a multifunctional receptor regulating diverse developmental processes. *Int. J. Biochem. Cell Biol.* 39:1569–1575.
37. Rajagopalan, S., L. Deitinghoff, D. Davis, S. Conrad, T. Skutella, A. Chedotal, B.K. Mueller, and S.M. Strittmatter. 2004. Neogenin mediates the action of repulsive guidance molecule. *Nat. Cell Biol.* 6:756–762.
38. Llambi, F., F.C. Lourenco, D. Gozuacik, C. Guix, L. Pays, G. Del Rio, A. Kimchi, and P. Mehlen. 2005. The dependence receptor UNC5H2 mediates apoptosis through DAP-kinase. *EMBO J.* 24:1192–1201.
39. Ferrandis, E., J. Da Silva, G. Riou, and J. Benard. 1994. Coactivation of the MDR1 and MYCN genes in human neuroblastoma cells during the metastatic process in the nude mouse. *Cancer Res.* 54:2256–2261.
40. Link, B.C., U. Reichelt, M. Schreiber, J.T. Kaifi, R. Wachowiak, D. Bogoevski, M. Bubenheim, G. Cataldegirmen, K.A. Gawad, R. Issa, et al. 2007. Prognostic implications of Netrin-1 expression and its receptors in patients with adenocarcinoma of the pancreas. *Ann. Surg. Oncol.* 14:2591–2599.
41. Inbal, B., O. Cohen, S. Polak-Charcon, J. Kopolovic, E. Vadai, L. Eisenbach, and A. Kimchi. 1997. DAP kinase links the control of apoptosis to metastasis. *Nature.* 390:180–184.
42. Stupack, D.G., T. Teitz, M.D. Potter, D. Mikolon, P.J. Houghton, V.J. Kidd, J.M. Lahti, and D.A. Cheresh. 2006. Potentiation of neuroblastoma metastasis by loss of caspase-8. *Nature.* 439:95–99.
43. Yebra, M., A.M. Montgomery, G.R. Diaferia, T. Kaido, S. Silletti, B. Perez, M.L. Just, S. Hildbrand, R. Hurford, E. Florkiewicz, et al. 2003. Recognition of the neural chemoattractant Netrin-1 by integrins alpha6beta4 and alpha3beta1 regulates epithelial cell adhesion and migration. *Dev. Cell.* 5:695–707.
44. Park, K.W., D. Crouse, M. Lee, S.K. Karnik, L.K. Sorensen, K.J. Murphy, C.J. Kuo, and D.Y. Li. 2004. The axonal attractant Netrin-1 is an angiogenic factor. *Proc. Natl. Acad. Sci. USA.* 101:16210–16215.
45. Lu, X., F. Le Noble, L. Yuan, Q. Jiang, B. De Lafarge, D. Sugiyama, C. Breant, F. Claes, F. De Smet, J.L. Thomas, et al. 2004. The netrin receptor UNC5B mediates guidance events controlling morphogenesis of the vascular system. *Nature.* 432:179–186.
46. Nguyen, A., and H. Cai. 2006. Netrin-1 induces angiogenesis via a DCC-dependent ERK1/2-eNOS feed-forward mechanism. *Proc. Natl. Acad. Sci. USA.* 103:6530–6535.

47. Wilson, B.D., M. Ii, K.W. Park, A. Suli, L.K. Sorensen, F. Larrieu-Lahargue, L.D. Urness, W. Suh, J. Asai, G.A. Kock, et al. 2006. Netrins promote developmental and therapeutic angiogenesis. *Science*. 313:640–644.
48. Jiang, Y., L. Min-tsai, and M.D. Gershon. 2003. Netrins and DCC in the guidance of migrating neural Crest-derived cells in the developing bowel and pancreas. *Dev. Biol.* 258:364–384.
49. Roperch, J.P., K. El Ouadrani, A. Hendrix, S. Emami, O. De Wever, G. Melino, and C. Gespach. 2008. Netrin-1 induces apoptosis in human cervical tumor cells via the TAp73alpha tumor suppressor. *Cancer Res.* 68:8231–8239.
50. Bourhis, J., C. Dominici, H. McDowell, G. Raschella, G. Wilson, M.A. Castello, E. Plouvier, J. Lemerle, G. Riou, J. Benard, et al. 1991. N-myc genomic content and DNA ploidy in stage IVS neuroblastoma. *J. Clin. Oncol.* 9:1371–1375.
51. Rubie, H., D. Plantaz, C. Coze, J. Michon, D. Frappaz, M.C. Baranzelli, P. Chastagner, M.C. Peyroulet, and O. Hartmann. 2001. Localised and unresectable neuroblastoma in infants: excellent outcome with primary chemotherapy. Neuroblastoma Study Group, Societe Francaise d'Oncologie Pediatrique. *Med. Pediatr. Oncol.* 36:247–250.
52. Ambros, I.M., J. Benard, M. Boavida, N. Bown, H. Caron, V. Combaret, J. Couturier, C. Darnfors, O. Delattre, J. Freeman-Edward, et al. 2003. Quality assessment of genetic markers used for therapy stratification. *J. Clin. Oncol.* 21:2077–2084.
53. Ghoumari, A.M., R. Wehrle, O. Bernard, C. Sotelo, and I. Dusart. 2000. Implication of Bcl-2 and Caspase-3 in age-related Purkinje cell death in murine organotypic culture: an in vitro model to study apoptosis. *Eur. J. Neurosci.* 12:2935–2949.
54. Vandesompele, J., K. De Preter, F. Pattyn, B. Poppe, N. Van Roy, A. De Paepe, and F. Speleman. 2002. Accurate normalization of real-time quantitative RT-PCR data by geometric averaging of multiple internal control genes. *Genome Biol.* 3:research0034.1–0034.11.
55. Gotoh, T., H. Hosoi, T. Iehara, Y. Kuwahara, S. Osone, K. Tsuchiya, M. Ohira, A. Nakagawara, H. Kuroda, and T. Sugimoto. 2005. Prediction of MYCN amplification in neuroblastoma using serum DNA and real-time quantitative polymerase chain reaction. *J. Clin. Oncol.* 23:5205–5210.
56. Schneider, T., F. Osl, T. Friess, H. Stockinger, and W. Scheuer. 2002. Quantification of human Alu sequences by real-time PCR—an improved method to measure therapeutic efficacy of anti-metastatic drugs in human xenotransplants. *Clin. Exp. Metastasis.* 19:571–582.

Biochemical and Biophysical Research Communications 390 (2009) 21–26

Contents lists available at ScienceDirect

Biochemical and Biophysical Research Communications

journal homepage: www.elsevier.com/locate/ybbrc

Positive auto-regulation of *MYCN* in human neuroblastoma

Yusuke Suenaga [a,b], Yoshiki Kaneko [a,b], Daisuke Matsumoto [a,c], Mohammad Shamim Hossain [a], Toshinori Ozaki [b,d], Akira Nakagawara [a,b,*]

[a] Division of Biochemistry and Innovative Cancer Therapeutics, Chiba Cancer Center Research Institute, Nitona, Chuoh-ku, Chiba 260-8717, Japan
[b] Department of Molecular Biology and Oncology, Graduate School of Medicine, Chiba University, Nitona, Chuoh-ku, Chiba 260-8717, Japan
[c] Department of Medical Engineering, Suzuka University of Medical Science, Kishioka, Suzuka 1001-1, Japan
[d] Laboratory of Anti-tumor Research, Chiba Cancer Center Research Institute, 666-2 Nitona, Chuoh-ku, Chiba 260-8717, Japan

ARTICLE INFO

Article history:
Received 10 September 2009
Available online 18 September 2009

Keywords:
MYCN
Neuroblastoma
Neuronal differentiation
All-*trans*-retinoic acid (ATRA)
Positive auto-regulation

ABSTRACT

MYCN oncogene is one of the most important regulators affecting the prognosis of neuroblastoma and is frequently amplified in the high-risk subsets. Despite its clinical significance, it remains unclear how the *MYCN* expression is regulated in human neuroblastomas. Here, we found the presence of a positive auto-regulatory mechanism of *MYCN*. Enforced expression of MYCN induced endogenous *MYCN* mRNA expression in SK-N-AS neuroblastoma cells with a single copy of *MYCN* gene. Luciferase reporter assay revealed that MYCN protein activates its own promoter activity in a dose-dependent manner and the downstream region relative to the transcription start sites is responsible for the activation. Furthermore, ChIP analysis showed that MYCN is directly recruited onto the intron 1 region of *MYCN* gene which contains two putative E-box sites. Intriguingly, in response to all-*trans*-retinoic acid (ATRA), MYCN was down-regulated in *MYCN*-amplified SK-N-BE neuroblastoma cells, and the recruitment of MYCN protein onto its own intron 1 region was reduced in association with an induction of neuronal differentiation. Collectively, our present results suggest that MYCN contributes to its own expression by forming a positive auto-regulatory loop in neuroblastoma cells.

Introduction

Neuroblastoma is one of the most common solid tumors in children and originates from the embryonic neural crest cells [1,2]. It accounts for about 15% of childhood cancer deaths, and at least 40% of all neuroblastomas are designated as high-risk tumors which often occur in patients over one year of age and show characteristic genomic abnormalities including allelic loss of the distal part of chromosome 1 and gain of chromosome 2p [1–3]. *MYCN* is an oncogene mapped to chromosome 2p, and its amplification is a strong indicator for poor outcome in patients' survival [4–6]. Transgenic mice which overexpress *MYCN* driven by the tyrosine hydroxylase promoter in sympathetic neurons develop aggressive neuroblastoma, indicating that *MYCN* has an intrinsic oncogenic potential *in vivo* [7]. MYCN protein activates transcription of the genes that are involved in diverse cellular function, such as cell growth, apoptosis, and differentiation [8,9]. Recently, by using computational analysis of gene expression profile, Fredlund et al. showed that high transcriptional activity of MYC family pathway in primary neuroblastomas predicts poor outcome of the patients and is correlated with low grade of neuronal differentiation in tumors [10]. These results are consistent with the notion that MYCN promotes tumor progression via transcriptional activation of the target genes, and that down-regulation of MYCN may be a critical step for the process of neuronal differentiation. Indeed, in response to differentiation stimuli like NGF or retinoic acids (RAs), endogenous expression of MYCN is suppressed [11,12] and enforced expression of MYCN inhibits NGF- or retinoic acid-mediated neuronal differentiation [13,14]. Moreover, MYCN silencing alone is enough to induce neuronal differentiation in several *MYCN*-amplified neuroblastoma cell lines [15,16].

Retinoic acids (RAs) are now being used as one of the tools in the standard treatment protocols for high risk neuroblastomas, and demonstrated significant therapeutic effects on event-free survival [1,17,18]. Although the down-regulation of MYCN by RA was first reported in 1985 [12], the precise mechanism of its regulation is still elusive [19]. Previously, E2F family and Sp1/Sp3 were reported as the transcription factors which regulate basal expression of MYCN [20–22]. In response to retinoic acid treatment, binding of E2F-2, -3 and -4 to the core promoter of *MYCN* gene was decreased after 12 days of RA treatment [20], whereas Sp1/Sp3 binding was not affected by RA [23]. However, since RA treatment represses *MYCN* transcription at more early stage [12], there might

* Corresponding author. Address: Division of Biochemistry and Innovative Cancer Therapeutics, Chiba Cancer Center Research Institute, 666-2 Nitona, Chuoh-ku, Chiba 260-8717, Japan. Fax: +81 43 265 4459.
E-mail address: akiranak@chiba-cc.jp (A. Nakagawara).

0006-291X/$ - see front matter © 2009 Published by Elsevier Inc.
doi:10.1016/j.bbrc.2009.09.044

be alternative mechanisms which accelerate a decline of *MYCN* mRNA in response to RA treatment.

In the present study, we have found the presence of a positive auto-regulation in *MYCN* transcription. MYCN protein enhances its own promoter activity through its direct recruitment onto the intron 1 region of *MYCN* gene. Treatment with all-*trans*-retinoic acid (ATRA) significantly represses *MYCN* mRNA expression accompanied by a marked decrease of the amount of MYCN protein recruited onto the intron 1 region. These results suggest that the positive auto-regulation of MYCN is repressed by ATRA, resulting in the further down-regulation of *MYCN* mRNA expression.

Materials and methods

Cell culture and transfection. SK-N-AS neuroblastoma cells were grown in RPMI 1640 medium supplemented with 10% heat-inactivated fetal bovine serum (FBS, Invitrogen) and antibiotic mixture in a humidified atmosphere of 5% CO_2 in air at 37 °C. SK-N-BE neuroblastoma cells were cultured in a mixture of minimal essential medium (MEM) and Hanks F12 medium supplemented with 15% heat-inactivated FBS and antibiotics. For transfection, cells were transfected with the indicated expression plasmids using Lipofectamine 2000 according to the manufacturer's instructions (Invitrogen).

Construction of luciferase reporter plasmids. A luciferase reporter plasmid containing the region of *MYCN* promoter encompassing from −221 to +1312 (where +1 represents the transcription initiation site) was generated by PCR-based amplification using genomic DNA prepared from human placenta as a template. Oligonucleotide primers used were as follows: 5′-GAGCTCCAGCTTTGCAGCCTTCTC-3′ (forward) and 5′-AACCAGGTTCCCCAATCTTC-3′ (reverse). An underlined sequence in the forward primer indicate the SacI restriction site. PCR products were subcloned into pGEMT Easy plasmid (Promega) according to the manufacturer's protocol. After sequencing, PCR products were digested with SacI and subcloned into SacI restriction sites of pGL3 basic plasmid (Promega) to give MYCN(−221/+1312).

RT-PCR and quantitative real-time RT-PCR. Total RNA was prepared using RNeasy Mini Kit (Qiagen) following the manufacturer's protocol. cDNA was synthesized using SuperScript II with random primers (Invitrogen). Quantitative real-time RT-PCR using an ABI PRISM 7500 System (Perkin-Elmer Applied Biosystems) was carried out according to the manufacturer's protocol. Following were primers used for this analysis: human *MYCN* 5′-TCCATGACAGCGCT AAACGTT-3′ (forward) and 5′-GGAACACACAAGGTGACTTCAACA-3′ (reverse). All the reactions were performed in triplicate. The mRNA levels of each of the genes were standardized by β-actin.

Immunoblotting. Cells were washed with ice-cold PBS and lysed with SDS-sample buffer. After a brief sonication, cell lysates were boiled for 5 min, resolved by 15% SDS–PAGE, and electrotransferred onto Immobilon-P membranes (Millipore). The membranes were blocked with Tris-buffered saline (TBS) containing 0.1% Tween 20 and 5% nonfat dry milk, and then incubated with monoclonal anti-MYCN (AB1, Oncogene Research Products), monoclonal anti-tTG (AB-3, NeoMarker), anti-TUBBIII (TuJ1, Covance), or with polyclonal anti-actin (20–33, Sigma) antibody for 1 h at room temperature, followed by an incubation with an appropriate horseradish peroxidase-conjugated secondary antibody (Jackson ImmunoResearch Laboratories) for 1 h at room temperature. The chemiluminescence reaction was performed using the ECL reagent (Amersham Biosciences).

Luciferase reporter assay. SK-N-AS cells were co-transfected with the indicated *MYCN* promoter luciferase reporters, pRL-TK *Renilla* luciferase cDNA together with or without the increasing amounts of the expression plasmid for MYCN. Total DNA per transfection was kept constant (510 ng) with pcDNA3 (Invitrogen). Forty-eight hours after transfection, firefly and *Renilla* luciferase activities were measured with Dual-luciferase reporter assay system according to the manufacturer's instructions (Promega).

Cell counting. Cells were seeded at a density of 10,000 cells/well in 12-well tissue culture plates. After allowing the attachment of cells overnight, culture medium was replaced with the fresh medium containing with or without 5 μM of ATRA. At the indicated time periods after ATRA treatment, the numbers of viable cells were measured in triplicate under microscopic observation.

Chromatin immunoprecipitation (ChIP) assay. ChIP assay was performed according to the protocol provided by Upstate Biotechnology. In brief, SK-N-BE cells were treated with or without 5 μM of ATRA for 3 days, and cells were cross-linked with 1% formaldehyde in medium at 37 °C for 8 min. Cells were then washed in ice-cold PBS and resuspended in 200 μl of SDS lysis buffer containing protease inhibitor mixture. The suspension was sonicated to an average length of 200–600 nucleotides, and pre-cleared with protein G-agarose beads for 30 min at 4 °C. The beads were removed by centrifugation and the chromatin solution was immunoprecipitated with normal mouse serum (NMS) or with monoclonal anti-MYCN (AB1, Oncogene Research Products) antibody at 4 °C overnight, followed by incubation with protein G-agarose beads for an additional 1 h at 4 °C. The immune complexes were eluted with 100 μl of elution buffer (1% SDS and 0.1 M $NaHCO_3$) and formaldehyde cross-links were reversed by heating at 65 °C for 6 h. Proteinase K was added to the reaction mixtures and incubated at 45 °C for 1 h. DNA of the immunoprecipitates and control input DNA were purified and then analyzed by standard PCR. Primers used were as follows: *MYCN*: forward 5′-CTGTCGTAGACAGCTTGTAC-3′, reverse 5′-AACCAGGTTCCCCAATCTTC-3′; *NLRR1*: forward 5′-AAGTT GGATTTGATGACTGATACG-3′, reverse 5′-AGGCAAGAGACCATGTGC AGGAG-3′. *NLRR1* was used as a positive control [24].

Results

MYCN enhances its own promoter activity

To examine whether MYCN could directly regulate its own expression in neuroblastoma cells, human neuroblastoma-derived SK-N-AS cells bearing a single copy of *MYCN*, were transiently transfected with MYCN expression plasmid and the expression levels of endogenous *MYCN* mRNA were measured by semi-quantitative RT-PCR. The primer set used in this study was designed to detect the 3′UTR region of *MYCN* mRNA. Therefore, only the endogenous *MYCN* mRNA was detectable. As shown in Fig. 1A, enforced expression of MYCN significantly induced the endogenous *MYCN* mRNA. Lower panel of Fig. 1A showed the results obtained from immunoblotting experiments. Under our experimental conditions, our antibody against MYCN detected both the endogenous and exogenous MYCN. Similar results were also obtained from the quantitative real-time RT-PCR (Fig. 1B), suggesting that MYCN has an ability to transactivate its own promoter.

To identify the MYCN-responsive region within human *MYCN* genomic sequence, we generated a luciferase reporter plasmid containing *MYCN* genomic fragment encompassing from −221 to +1312, where +1 represents the transcriptional initiation site, termed MYCN(−221/+1312). SK-N-AS cells were transiently co-transfected with the constant amount of MYCN(−221/+1312), *Renilla* luciferase reporter plasmid together with or without the increasing amounts of the expression plasmid for MYCN. As shown in Fig. 1C, enforced expression of MYCN resulted in a significant enhancement of the luciferase activity driven by *MYCN* promoter in a dose-dependent manner. These results strongly suggest that the genomic fragment of *MYCN* (at positions −221 to +1312) contains a MYCN-responsive region(s).

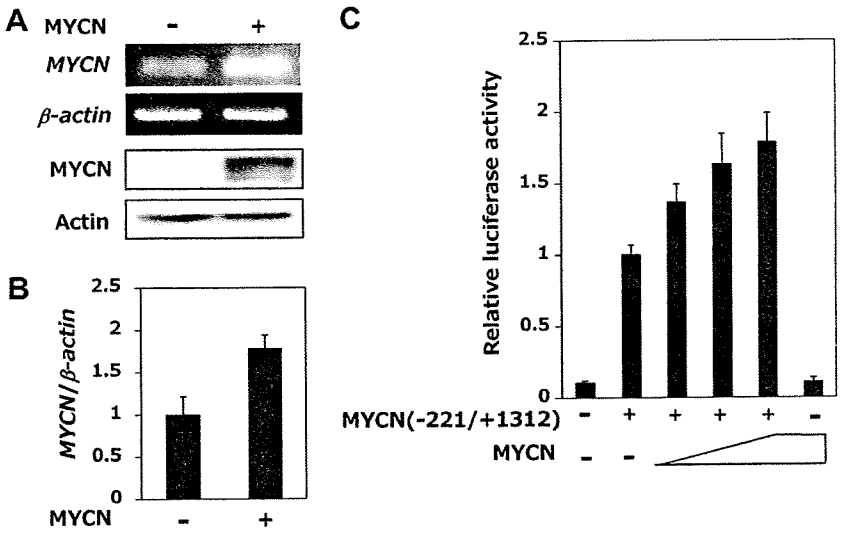

Fig. 1. Enforced expression of MYCN induces the endogenous *MYCN* mRNA. (A) Expression levels of the endogenous *MYCN* mRNA. SK-N-AS neuroblastoma cells were transiently transfected with pcDNA3 or with MYCN expression plasmid. Forty-eight hours after transfection, total RNA and whole cell lysates were prepared and subjected to semi-quantitative RT-PCR and immunoblotting, respectively. For RT-PCR, β-actin was used as an internal control. For immunoblotting, actin was used as a loading control. (B) Quantitative real-time RT-PCR. Total RNA were prepared as in (A) and subjected to quantitative real-time RT-PCR to examine the expression levels of the endogenous *MYCN* mRNA. (C) Luciferase reporter assay. SK-N-AS cells were transiently co-transfected with the constant amount of the luciferase reporter plasmid termed MYCN(−221/+1312) (100 ng) and *Renilla* luciferase reporter plasmid (pRL-TK) (10 ng) along with or without the increasing amounts of MYCN expression plasmid (100, 200, or 400 ng). Forty-eight hours after transfection, cells were lysed and their luciferase activities were measured. Firefly luminescence signal was standardized by the *Renilla* luminescence signal. Results are shown as fold induction of the firefly luciferase activity compared with control cells transfected with the empty plasmid.

MYCN is recruited onto the putative E-boxes located within intron 1 of MYCN to enhance its own promoter activity

During an extensive search for the 5′-upstream region and intron 1 of human *MYCN*, we have found out two canonical E-boxes within intron 1. We then generated two kinds of 3′-trucated *MYCN* promoter luciferase reporter constructs termed MYCN(−1030/+21) and MYCN(−221/+21) and determined their luciferase activities in response to ectopic MYCN. As shown in Fig. 2A, the luciferase reporter assay demonstrated that both of those luciferase reporter constructs do not respond to the increasing amounts of MYCN, suggesting that the genomic fragment (at positions +22 to +1312) containing the putative E-boxes but not the 5′-upstream region of *MYCN* is required for MYCN-dependent transcriptional activation of *MYCN*.

To further confirm this notion, we performed a chromatin immunoprecipitation (ChIP) assay. The cross-linked genomic DNA prepared from *MYCN*-amplified human neuroblastoma-derived SK-N-BE cells was subjected to ChIP assay using the indicated primer set (Fig. 2B). *NLRR1* which is one of MYCN-target gene [24], was employed as a positive control for this experiment. As clearly shown in Fig. 2B, DNA fragment containing the putative E-boxes was specifically amplified, indicating that the endogenous MYCN directly binds to the canonical E-boxes.

ATRA induces neuronal differentiation in SK-N-BE cells

All-*trans*-retinoic acid (ATRA) is one of the well-established inducers for neuronal differentiation and/or apoptosis in neuroblastoma cells. In response to ATRA, a marked reduction in the expression level of *MYCN* is detectable in neuroblastoma-derived cell lines [8]. Consistent with those observations, ATRA treatment resulted in a significant decrease in growth rate of SK-N-BE cells (Fig. 3A) in association with their remarkable morphological changes (Fig. 3B). Close inspection of cell shapes demonstrated that

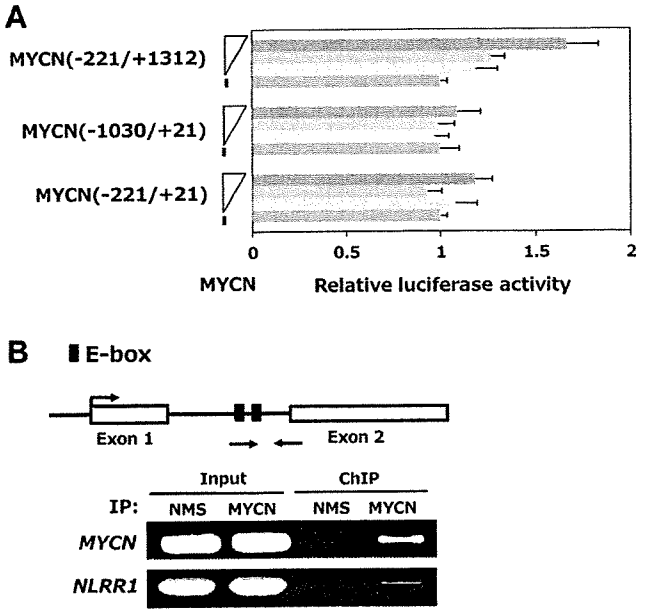

Fig. 2. MYCN has an ability to enhance its own promoter activity. (A) Luciferase reporter assay. SK-N-AS cells were transiently co-transfected with the constant amount of the indicated luciferase reporter constructs (100 ng) and *Renilla* luciferase reporter plasmid (pRL-TK) (10 ng) together with the empty plasmid (pcDNA3) or with the expression plasmid for MYCN. Forty-eight hours after transfection, cells were lysed and their luciferase activities were measured as in Fig. 1C. (B) ChIP assay. SK-N-BE neuroblastoma cells were cross-linked with formaldehyde and the cross-linked chromatin was sonicated followed by immunoprecipitation with normal mouse serum (NMS) or with monoclonal anti-MYCN antibody. Genomic DNA was purified from the immunoprecipitates and subjected to PCR using the indicated primer set. The positions of the putative E-boxes and primer set are also shown. The anti-NLRR1 immunoprecipitates were used as a positive control.

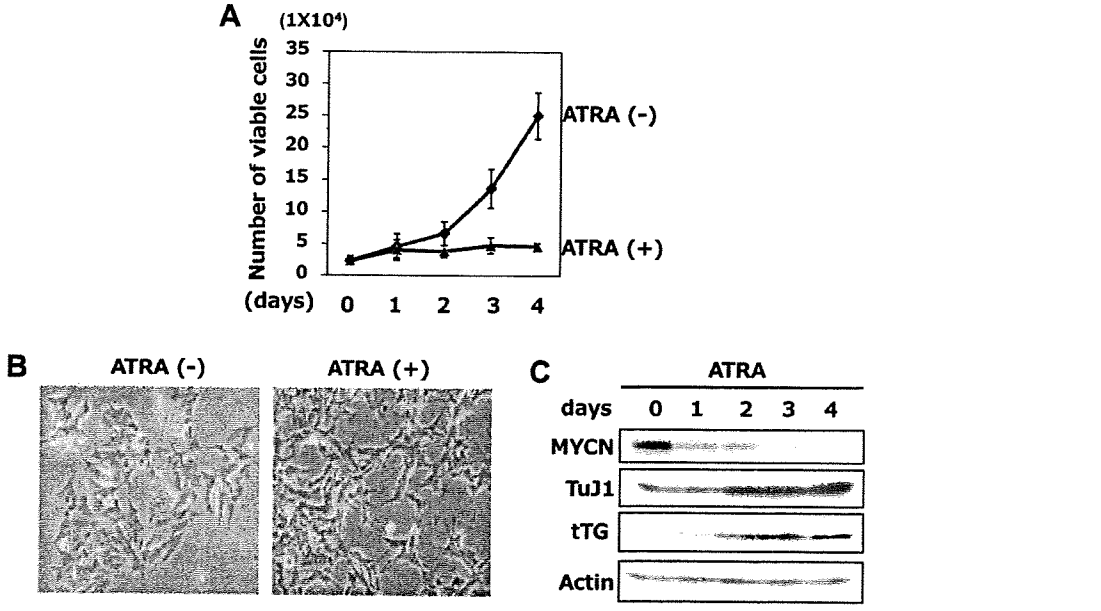

Fig. 3. ATRA induces neuronal differentiation in SK-N-BE cells. (A) Growth curves of SK-N-BE cells in the presence (solid diamond) or absence (solid triangle) of ATRA. Cells were grown in the standard culture medium and treated with 5 μM of ATRA or left untreated. At the indicated time points after the treatment with ATRA, number of viable cells was measured in triplicate. (B) ATRA-mediated neuronal differentiation in SK-N-BE cells. Cells were exposed to ATRA at a final concentration of 5 μM or left untreated. Four days after the treatment with ATRA, cells were examined by phase-contrast microscopy. (C) Immunoblotting. SK-N-BE cells were exposed to 5 μM of ATRA. At the indicated time periods after ATRA treatment, whole cell lysates were prepared and processed for immunoblotting with the indicated antibodies. Actin was used as a loading control.

ATRA treatment induces neurite outgrowth, suggesting that SK-N-BE cells undergo neuronal differentiation in response to ATRA. Additionally, ATRA-mediated down-regulation of the endogenous MYCN and concomitant up-regulation of neuronal markers such as neuron specific class III β-tubulin (TuJ1) [25] as well as transglutaminase II (tTG) [26] were detected as examined by immunoblotting (Fig. 3C).

A significant decrease in the amounts of MYCN recruited onto the genomic region containing the putative E-boxes in response to ATRA

We then examined the expression levels of *MYCN* mRNA in ATRA-treated SK-N-BE cells. To this end, SK-N-BE cells were exposed to 5 μM of ATRA. At the indicated time points after ATRA treatment, total RNA was prepared and processed for quantitative real-time RT-PCR. In accordance with previous observations [12], the expression levels of the endogenous *MYCN* mRNA significantly decreased in ATRA-treated SK-N-BE cells (Fig. 4A, upper panel). Similar results were also obtained from semi-quantitative RT-PCR (Fig. 4A, lower panel). These observations prompted us to examine whether MYCN could be involved in a decrease in *MYCN* mRNA levels in response to ATRA. For this purpose, we performed ChIP assays using ATRA-treated SK-N-BE cells. As shown in Fig. 4B, ATRA treatment remarkably reduced the amounts of the endogenous MYCN recruited onto the genomic region containing the putative E-boxes. Since MYCN enhanced its own promoter activity, our present findings indicate that ATRA-mediated decrease in the expression level of the endogenous MYCN leads to the repression of the positive auto-regulation of MYCN, and thereby promoting neuronal differentiation.

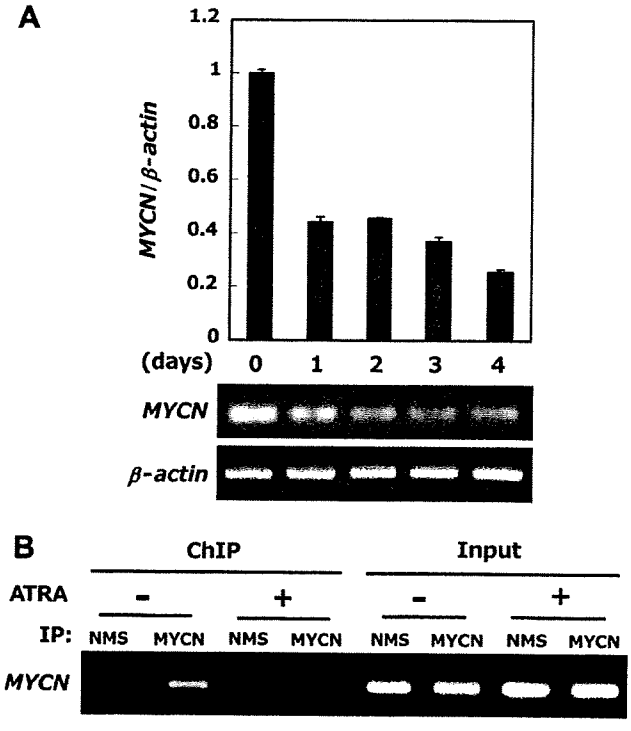

Fig. 4. ATRA-mediated down-regulation of *MYCN* mRNA. (A) Quantitative real-time and semi-quantitative RT-PCR. SK-N-BE cells were treated with 5 μM ATRA. At the indicated time periods after the treatment with ATRA, total RNA were prepared and subjected to quantitative real-time RT-PCR (upper panel) and semi-quantitative RT-PCR (lower panel). *β-actin* was used as an internal control. (B) ChIP assay. SK-N-BE cells were treated with 5 μM of ATRA or left untreated. Three days after ATRA treatment, cells were cross-linked with formaldehyde. The cross-linked chromatin was sonicated and immunoprecipitated with normal mouse serum (NMS) or with monoclonal anti-MYCN antibody. Genomic DNA was then purified from the immunoprecipitates and subjected to PCR-based amplification by using the primer set as shown in Fig. 2B.

Discussion

Similarly to other MYC family members, c-*MYC* and *MYCL*, the *MYCN* gene is frequently amplified in many types of human cancers including neuroblastoma, and its overexpression is significantly associated with aggressiveness of the tumors [1,27]. In

neuroblastoma, *MYCN* is amplified and closely linked to poor survival probability of patients [4–6]. However, expression levels of *MYCN* in individual tumors are regulated by not only the gene copy number but also the transcriptional regulation [28,29]. Indeed, *MYCN* mRNA is expressed at significantly high levels even in some subsets of neuroblastoma with a single copy number of *MYCN* gene. In the present study, we have demonstrated that MYCN protein enhances its own promoter activity through direct binding to the intron 1 region. To our knowledge, this is the first evidence that MYCN forms a positive auto-regulatory loop through its own transcriptional activation. Since the amplified genomic DNA at *MYCN* gene contains the responsive MYCN binding sites (within intron 1), the identified mechanism may explain the reason why transcription of each *MYCN* gene is activated both in *MYCN*-amplified and non-amplified neuroblastoma cells.

In a sharp contrast to *c-MYC*, the expression of *MYCN* is strictly restricted in both human and mouse adult tissues [9,19,30]. To delineate the essential region of *MYCN* promoter for the tissue-specific expression, the previous studies using transgenic mice showed that the human transgene containing 3.5 kb of upstream and 3 kb of downstream sequences were, at least in part, responsible for the expression pattern of the endogenous *MYCN* gene [31,32]. Further studies revealed that the downstream region including exon 1 and intron 1 is required for tissue-specific promoter activity of *MYCN*, whereas the upstream region regulates basal promoter activity [19]. In support with this notion, the latter region includes a sequence with high homology to the second promoter of *c-MYC*. Furthermore, E2F family proteins bind to enhance basal transcription activity through these regions in both of the two genes [19,20]. Our present results have also revealed that ectopically expressed MYCN activates its own promoter activity through the intron 1 region but not the upstream region, suggesting that the positive auto-regulation of *MYCN* may contribute to maintain tissue-specific expression of *MYCN* rather than basal transcription of the gene.

We have previously found that endogenous expression level of Bcl-2 is one of the keys to determine responsiveness to ATRA for inducing neuronal differentiation or apoptosis in neuroblastoma cells [33]. Indeed, ATRA treatment repressed *MYCN* expression and thereby cells underwent differentiation or apoptotic cell death [12,19]. However, it has been shown that *MYCN* mRNA is transiently down-regulated in response to RA and begins to increase 3–4 days after the administration of RA in several RA-resistant neuroblastoma cell lines [34 and our unpublished observations]. Therefore, it is likely that there could exist at least two distinct molecular mechanisms behind *MYCN* expression in response to RA. The first one is that *MYCN* expression is rapidly down-regulated in response to RA in RA-sensitive neuroblastoma cells. The second one is that RA-mediated repression of *MYCN* is recovered in RA-resistant neuroblastoma cells. Considering that MYCN has an ability to transactivate *MYCN* gene, it is conceivable that this positive auto-regulatory mechanism of *MYCN* expression might be at least in part involved in both cases. Thus, the disruption of this positive auto-regulatory mechanism of *MYCN* expression might provide a novel strategy for developing anti-cancer treatment. To date, it remains unclear how ATRA treatment could cause the down-regulation of *MYCN* in ATRA-sensitive neuroblastoma cells. Further studies should be required to address this issue.

Acknowledgments

This work was supported in part by a Grant-in-Aid from the Ministry of Health, Labor and Welfare for Third Term Comprehensive Control Research for Cancer, a Grant-in-Aid for Scientific Research on Priority Areas from the Ministry of Education, Culture, Sports, Science and Technology, Japan, a Grant-in-Aid for Scientific Research from Japan Society for the Promotion of Science, grants from Uehara Memorial Foundation, a Global COE Program (Global Center for Education and Research in Immune System Regulation and Treatment), Graduate School of Medicine, Chiba University. The authors thank Ms. Mami Yamamoto for technical assistance and Dr. Kiyohiro Ando for valuable discussions.

References

[1] G.M. Brodeur, Neuroblastoma: biological insights into a clinical enigma, Nat. Rev. Cancer 3 (2003) 203–216.
[2] A. Nakagawara, M. Ohira, Comprehensive genomics linking between neural development and cancer: neuroblastoma as a model, Cancer Lett. 204 (2004) 213–224.
[3] N. Tomioka, S. Oba, M. Ohira, A. Misra, J. Fridlyand, S. Ishii, Y. Nakamura, E. Isogai, T. Hirata, Y. Yoshida, S. Todo, Y. Kaneko, D.G. Albertson, D. Pinkel, B.G. Feuerstein, A. Nakagawara, Novel risk stratification of patients with neuroblastoma by genomic signature, which is independent of molecular signature, Oncogene 27 (2008) 441–449.
[4] G.M. Brodeur, R.C. Seeger, M. Schwab, H.E. Varmus, J.M. Bishop, Amplification of N-myc in untreated human neuroblastomas correlates with advanced disease stage, Science 224 (1984) 1121–1124.
[5] M. Schwab, J. Ellison, M. Busch, W. Rosenau, H.E. Varmus, J.M. Bishop, Enhanced expression of the human gene N-myc consequent to amplification of DNA may contribute to malignant progression of neuroblastoma, Proc. Natl. Acad. Sci. USA 81 (1984) 4940–4944.
[6] R.C. Seeger, G.M. Brodeur, H. Sather, A. Dalton, S.E. Siegel, K.Y. Wong, D. Hammond, Association of multiple copies of the N-myc oncogene with rapid progression of neuroblastomas, N. Engl. J. Med. 313 (1985) 1111–1116.
[7] W.A. Weiss, K. Aldape, G. Mohapatra, B.G. Feuerstein, J.M. Bishop, Targeted expression of MYCN causes neuroblastoma in transgenic mice, EMBO J. 16 (1997) 2985–2995.
[8] N. Meyer, L.Z. Penn, Reflecting on 25 years with MYC, Nat. Rev. Cancer 8 (2008) 976–990.
[9] M. Eilers, R.N. Eisenman, Myc's broad reach, Genes Dev. 22 (2008) 2755–2766.
[10] E. Fredlund, M. Ringnér, J.M. Maris, S. Påhlman, High Myc pathway activity and low stage of neuronal differentiation associate with poor outcome in neuroblastoma, Proc. Natl. Acad. Sci. USA 105 (2008) 14094–14099.
[11] H. Matsushima, E. Bogenmann, Expression of trkA cDNA in neuroblastomas mediates differentiation in vitro and in vivo, Mol. Cell. Biol. 13 (1993) 7447–7456.
[12] C.J. Thiele, C.P. Reynolds, M.A. Israel, Decreased expression of N-myc precedes retinoic acid-induced morphological differentiation of human neuroblastoma, Nature 313 (1985) 404–406.
[13] E. Bogenmann, M. Torres, H. Matsushima, Constitutive N-myc gene expression inhibits trkA mediated neuronal differentiation, Oncogene 10 (1995) 1915–1925.
[14] F.A. Peverali, D. Orioli, L. Tonon, P. Ciana, G. Bunone, M. Negri, G. Della-Valle, Retinoic acid-induced growth arrest and differentiation of neuroblastoma cells are counteracted by N-myc and enhanced by max overexpressions, Oncogene 12 (1996) 457–462.
[15] A. Negroni, S. Scarpa, A. Romeo, S. Ferrari, A. Modesti, G. Raschellà, Decrease of proliferation rate and induction of differentiation by a MYCN antisense DNA oligomer in a human neuroblastoma cell line, Cell Growth Differ. 2 (1991) 511–518.
[16] J.H. Kang, P.G. Rychahou, T.A. Ishola, J. Oiao, B.M. Evers, D.H. Chung, MYCN silencing induces differentiation and apoptosis in human neuroblastoma cells, Biochem. Biophys. Res. Commun. 351 (2006) 192–197.
[17] R. Lotan, Retinoids in cancer chemoprevention, FASEB J. 10 (1996) 1031–1039.
[18] K.K. Matthay, J.G. Villablanca, R.C. Seeger, D.O. Stram, R.E. Harris, N.K. Ramsay, P. Swift, H. Shimada, C.T. Black, G.M. Brodeur, R.B. Gerbing, C.P. Reynolds, Treatment of high-risk neuroblastoma with intensive chemotherapy, radiotherapy, autologous bone marrow transplantation, and 13-cis-retinoic acid. Children's Cancer Group, N. Engl. J. Med. 341 (1999) 1165–1173.
[19] V. Strieder, W. Lutz, Regulation of N-myc expression in development and disease, Cancer Lett. 180 (2002) 107–109.
[20] V. Strieder, W. Lutz, E2F proteins regulate MYCN expression in neuroblastomas, J. Biol. Chem. 278 (2003) 2983–2989.
[21] T.H. Inge, L.K. Casson, W. Priebe, J.O. Trent, K.E. Georgeson, D.M. Miller, P.J. Bates, Importance of Sp1 consensus motifs in the MYCN promoter, Surgery 132 (2002) 232–238.
[22] C. Kramps, V. Strieder, A. Sapetschnig, G. Suske, W. Lutz, E2F and Sp1/Sp3 synergize but are not sufficient to activate the MYCN gene in neuroblastomas, J. Biol. Chem. 279 (2004) 5110–5117.
[23] K.K. Kanemaru, M.C. Tuthill, K.K. Takeuchi, N. Sidell, R.K. Wada, Retinoic acid induced downregulation of MYCN is not mediated through changes in Sp1/Sp3, Pediatr. Blood Cancer 50 (2008) 806–811.
[24] M.S. Hossain, T. Ozaki, H. Wang, A. Nakagawa, H. Takenobu, M. Ohira, T. Kamijo, A. Nakagawara, N-MYC promotes cell proliferation through a direct transactivation of neuronal leucine-rich repeat protein-1 (NLRR1) gene in neuroblastoma, Oncogene 27 (2008) 6075–6082.
[25] E. Dráberová, Z. Lukás, D. Ivanyi, V. Viklický, P. Dráber, Expression of class III beta-tubulin in normal and neoplastic human tissues, Histochem. Cell Biol. 109 (1998) 231–239.

[26] J. Tucholski, M. Lesort, G.V. Johnson, Tissue transglutaminase is essential for neurite outgrowth in human neuroblastoma SH-SY5Y cells, Neuroscience 102 (2001) 481–491.
[27] M. Schwab, MYCN in neuronal tumours, Cancer Lett. 204 (2004) 179–187.
[28] N.E. Kohl, C.E. Gee, F.W. Alt, Activated expression of the N-myc gene in human neuroblastomas and related tumors, Science 226 (1984) 1335–1337.
[29] R.K. Wada, R.C. Seeger, G.M. Brodeur, P.A. Einhorn, S.A. Rayner, M.M. Tomayko, C.P. Reynolds, Human neuroblastoma cell lines that express N-myc without gene amplification, Cancer 72 (1993) 3346–3354.
[30] P.J. Hurlin, N-Myc functions in transcription and development, Birth Defects Res. C Embryo Today 75 (2005) 340–352.
[31] K. Zimmerman, E. Legouy, V. Stewart, R. Depinho, F.W. Alt, Differential regulation of the N-myc gene in transfected cells and transgenic mice, Mol. Cell. Biol. 10 (1990) 2096–2103.
[32] S. Hiller, S. Breit, Z.Q. Wang, E.F. Wagner, M. Schwab, Localization of regulatory elements controlling human MYCN expression, Oncogene 6 (1991) 969–977.
[33] H. Niizuma, Y. Nakamura, T. Ozaki, H. Nakanishi, M. Ohira, E. Isogai, H. Kageyama, M. Imaizumi, A. Nakagawara, Bcl-2 is a key regulator for the retinoic acid-induced apoptotic cell death in neuroblastoma, Oncogene 25 (2006) 5046–5055.
[34] R.K. Wada, R.C. Seeger, C.P. Reynolds, T. Alloggiamento, J.M. Yamashiro, C. Ruland, A.C. Black, J.D. Rosenblatt, Cell type-specific expression and negative regulation by retinoic acid of the human N-myc promoter in neuroblastoma cells, Oncogene 7 (1992) 711–717.

Dysregulation of Platelet-Derived Growth Factor β-Receptor Expression by ΔNp73 in Neuroblastoma

Daniel Wetterskog,[1] Abtin Moshiri,[1] Toshinori Ozaki,[2] Hidetaka Uramoto,[1,3] Akira Nakagawara,[2] and Keiko Funa[1]

[1]Department of Medical Chemistry and Cell Biology, Institute of Biomedicine, Sahlgrenska Academy, University of Gothenburg, Gothenburg, Sweden; [2]Second Department of Surgery, University of Occupational and Environmental Health, Kitakyushu, Japan; and [3]Division of Biochemistry, Chiba Cancer Center Research Institute, Chiba, Japan

Abstract

We have previously characterized how p53 family proteins control the transcriptional regulation of the platelet-derived growth factor β-receptor (PDGFRB) and found that ΔNp73α, acting dominant-negatively to p53 and p73, can upregulate PDGFRB promoter activity. Here, we report that PDGFRB regulation differs between two neuroblastoma cell lines, correlating with the actions of ΔNp73. We found that PDGFRB was highly expressed in IMR-32 cells, and serum stimulation of IMR-32 cells did not downregulate PDGFRB expression, as seen in SH-SY5Y cells. In IMR-32, ΔNp73 was found constitutively bound to the PDGFRB promoter, and silencing of ΔNp73 resulted in repression of PDGFRB promoter activity as well as decreased PDGFRB protein expression. However, the anticancer drug cisplatin, known to stabilize and activate p53 and p73, downregulated PDGFRB expression not only in SH-SY5Y but also in IMR-32. Chromatin immunoprecipitation showed that cisplatin removed ΔNp73 from the PDGFRB promoter and recruited p53 and p73, leading to binding of histone deacetylase 4. These results suggest a direct role of ΔNp73 in the constantly enhanced PDGFRB expression seen in tumors. (Mol Cancer Res 2009;7(12):2031–9)

Introduction

The platelet-derived growth factor (PDGF) is known to play an important role in cellular proliferation (1). To prevent uncontrolled proliferation in response to PDGF stimulation, feedback mechanisms reduce PDGF receptors presented on the cell surface through ligand-mediated receptor endocytosis, receptor degradation, and transcriptional repression (2-6). Defective feedback mechanisms that cause deregulated PDGF signaling are implicated in various pathologic conditions, including cancer, where many tumors simultaneously express PDGF and its receptors at high levels (7, 8). This suggests the presence of an autocrine or paracrine PDGF stimulation of growth in such tumors.

We previously showed a key role for the p53 family in the feedback mechanisms that regulate PDGFRB transcription. Via their sterile α-motif, the p73 isoforms p73α and ΔNp73α bind the main transcriptional regulator of PDGFRB, NF-Y, where p73α mediates downregulation of PDGFRB and upregulation of ΔNp73α (9). Recently, we have reported that p53 as well as p73α/ΔNp73α are also able to directly bind the p53 consensus-like sequence on the promoter (10). Moreover, during cell cycle progression of normal cells, PDGFRB expression decreases on growth factor stimulation of G_1-G_0–arrested cells to prevent excess growth signals. For this functional regulation, dynamic interactions of the isoforms p73α and ΔNp73α with the PDGFRB promoter are important (11).

It is known that ΔNp73 isoforms are expressed in a number of human tumors including the most common solid tumor of early childhood, neuroblastoma, where ΔNp73α overexpression is associated with poor outcome (12-14). The status of p53 and p73 is also known to be of great importance for cancer progression, with mutations of p53 found in more than 50% of analyzed tumors (15). p73, on the other hand, is rarely found to be mutated, although its chromosomal region 1p36 is often deleted in human cancers and is the most common chromosomal abnormality observed in neuroblastoma (16, 17). The correlation between ΔNp73α and clinical outcome in neuroblastoma can be explained by the ability of ΔNp73 isoforms to act dominant-negatively to p53 and p73. ΔNp73 either competes with p53 or p73 for their DNA binding or binds to one of them, thereby inhibiting their respective transactivation activities (18-20). In this study, we have examined whether the status and actions of ΔNp73 and other p53 family members could explain the defective regulation of PDGFRB found in certain cancers.

To characterize the role of p53 family members in the transcriptional regulation of PDGFRB in neuroblastoma, we used two cell lines, IMR-32 and SH-SY5Y, which express both ΔNp73 and PDGFRB. We examined whether they respond similarly to two known stimuli resulting in PDGFRB downregulation (i.e., serum stimulation and cisplatin treatment). Many of the antitumor drugs used today induce and stabilize p53 and p73, thereby inducing p21 to arrest the cell cycle or promote

Received 10/23/08; revised 9/16/09; accepted 10/11/09; published OnlineFirst 12/1/09.

Grant support: The Swedish Science Council, Swedish Cancer Society, Swedish Children's Cancer Society, the Swedish Foundation for International Cooperation in Research and Higher Education, the Västra Götaland Health Service, the Royal Society of Arts and Sciences in Göteborg, the Lennander Foundation, and the Hjalmar Svensson Foundation.

The costs of publication of this article were defrayed in part by the payment of page charges. This article must therefore be hereby marked *advertisement* in accordance with 18 U.S.C. Section 1734 solely to indicate this fact.

Note: Supplementary data for this article are available at Molecular Cancer Research Online (http://mcr.aacrjournals.org/).

Requests for reprints: Keiko Funa, Department of Medical Chemistry and Cell Biology, Institute of Biomedicine, University of Gothenburg, Box 440, SE-405 30 Gothenburg, Sweden. Phone: 46-31-7863360; Fax: 46-31-416108. E-mail: keiko.funa@gu.se

doi:10.1158/1541-7786.MCR-08-0501

apoptosis (21, 22). Under these conditions, it is important that PDGFRB expression is downregulated to prevent continued proliferation. If members of the p53 family are inactivated (i.e., through mutations or a stable expression of a dominant-negative ΔNp73 isoform), then PDGFRB transcription might not be regulated normally.

We report here that addition of serum to serum-starved IMR-32 does not result in a downregulation of PDGFRB expression when ΔNp73 is constantly bound to the PDGFRB promoter. As expected, expression of small interfering RNA (siRNA) against ΔNp73 could induce the repression of the promoter activity and protein expression in IMR-32. In contrast, cisplatin treatment is able to remove ΔNp73 from the PDGFRB promoter, downregulating PDGFRB even in IMR-32.

Results

Serum Stimulation of IMR-32, Unlike SH-SY5Y, Does Not Repress PDGFRB Protein Expression or mRNA Levels

We assumed that the high expression of PDGFRB in neuroblastoma might be due to deranged p53 family proteins. Testing this assumption, we used serum stimulation to induce and/or activate p53 family proteins to detect changes in PDGFRB expression in IMR-32 and SH-SY5Y neuroblastoma cell lines. In

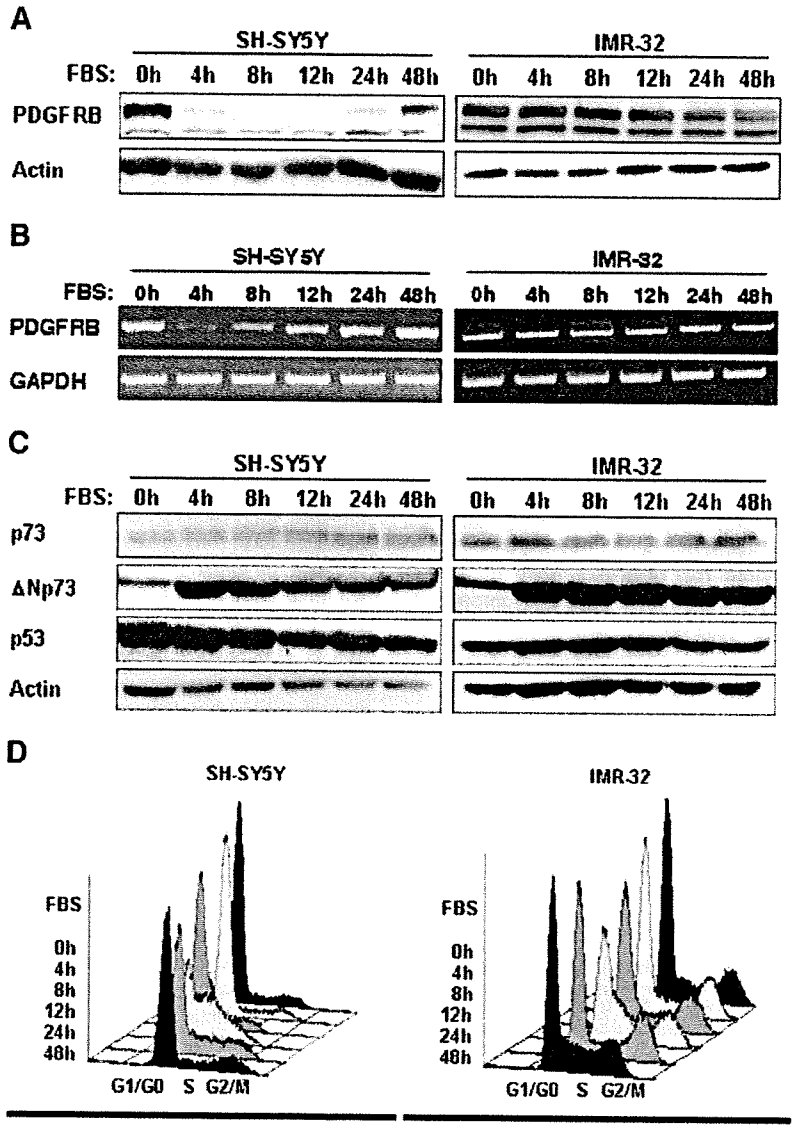

FIGURE 1. Dysregulated PDGFRB expression in IMR-32. SH-SY5Y and IMR-32 were serum starved for 48 h, and 10% FBS was added for 0, 4, 8, 12, 24, and 48 h until harvest. **A.** Serum stimulation of IMR-32, but not of SH-SY5Y, fails to repress PDGFRB protein expression. Cell lysates were immunoblotted with antibodies against PDGFRB and with actin as a standard. **B.** Serum stimulation of IMR-32, but not of SH-SY5Y, fails to repress PDGFRB mRNA expression. Reverse-transcribed PCR products of total RNA extracted from SH-SY5Y and IMR-32 are shown for PDGFRB and GAPDH. **C.** ΔNp73 is induced at high levels in both SH-SY5Y and IMR-32 on serum stimulation. Cell lysates were immunoblotted with antibodies against p73 (H-79), ΔNp73, p53 (DO1), and actin. **D.** Serum stimulation induces IMR-32 and SH-SY5Y cells to enter the cell cycle. Cellular DNA content was measured and analyzed with a flow cytometer. An FL2-H overlay is shown from cells gated to exclude debris and aggregated cells.

Table 1. Cell Cycle Analysis of SH-SY5Y and IMR32 following Serum Stimulation

	G_1-G_0	S	G_2-M
0 h	81.2 ± 0.1	10.9 ± 0.5	5.6 ± 0.1
4 h	79.3 ± 0.4	11.7 ± 1.7	6.7 ± 0.5
8 h	71.9 ± 1.7	20.0 ± 3.2	7.2 ± 2.7
12 h	45.1 ± 5.1	45.8 ± 0.8	7.5 ± 1.4
24 h	56.2 ± 1.7	28.0 ± 2.7	12.8 ± 0.3
48 h	69.4 ± 2.4	20.8 ± 3.8	8.3 ± 0.9
	G_1-G_0	S	G_2-M
0 h	57.6 ± 1.4	26.2 ± 2.9	13.8 ± 0.7
4 h	56.7 ± 3.1	24.4 ± 0.8	14.3 ± 0.4
8 h	55.1 ± 6.5	24.8 ± 0.4	16.2 ± 1.3
12 h	43.7 ± 3.0	31.6 ± 4.2	20.3 ± 7.0
24 h	51.9 ± 1.1	26.0 ± 1.4	20.1 ± 1.1
48 h	56.6 ± 3.8	26.2 ± 7.9	13.9 ± 1.7

serum-starved SH-SY5Y cells, addition of serum led to a 70% to 80% decrease in PDGFRB protein levels at 4 hours until 24 hours, which later increased at 48 hours. However, no such decrease was seen for IMR-32 (Fig. 1A; Supplementary Fig. S1).

We then examined whether differences in the observed PDGFRB regulation were reflected at the transcriptional level. Semiquantitative reverse transcription-PCR showed that PDGFRB mRNA expression in SH-SY5Y and IMR-32 correlated with changes in the respective protein level in response to adding serum, suggesting that the decrease of protein is a result of transcriptional changes rather than other feedback mechanisms such as protein internalization and degradation (Fig. 1B). Next, we compared the protein expression of the well-established transcriptional regulators of PDGFRB (p53, p73α, and ΔNp73α) between IMR-32 and SH-SY5Y to see if differences in their responses to serum stimulation could explain the differences in transcriptional regulation. As shown in Fig. 1C and Supplementary Fig. S1, the expression of p53 family members was similar between the cell lines. In both cell lines, an increase of ΔNp73α following serum addition was observed. Supplementary Fig. S2 shows a similar expression pattern of three isoforms of p73 and ΔNp73 at the protein levels in SH-SY5Y and IMR-32, although ΔNp73α mRNA is much more strongly expressed in IMR-32.

To confirm that serum stimulation induced both cell lines to leave the G_1 phase, fluorescence-activated cell sorting was run. For both cell lines, cells in the G_1 phase of the cell cycle decreased on serum stimulation, and cells in the S and G_2-M phases were increased to around 50% at maximum (Fig. 1D; Table 1). However, serum-starved IMR-32 cells had roughly twice as many cells in S and G_2-M as that for SH-SY5Y (40% and 16.5%, respectively).

Silencing of ΔNp73 Downregulates PDGFB Promoter Activity and Protein Levels in IMR-32, and ΔNp73 Is Found Bound to the Promoter Chromatin in IMR-32

We have previously shown that p53 family proteins regulate transcription of PDGFRB during the cell cycle (10, 11). Because we did not see any clear differences in p53, p73α, and ΔNp73α at protein levels (Fig. 1C), we assessed their ability to affect PDGFRB transcription. In agreement with our previous studies, analysis of PDGFRB promoter luciferase assays showed that both p53 and p73α repressed the promoter activity when compared with the vector control in both cell lines, whereas ΔNp73α activated the promoter (Fig. 2A). The role of ΔNp73 was further examined on the activity of PDGFRB promoter following cotransfection of an siRNA targeting ΔNp73. As shown in Fig. 2B, silencing of ΔNp73 reduced PDGFRB promoter activity by 60% in IMR-32, but not in SH-SY5Y, suggesting that the PDGFRB promoter is under the control of ΔNp73 in IMR-32 in normal condition. The silencing of ΔNp73 was confirmed for both cell lines, but only in IMR-32 was PDGFRB protein downregulated, thus further supporting that PDGFRB is controlled by ΔNp73 in this cell line (Fig. 2C)

To pinpoint differences in the *in vivo* recruitment of p53, p73, and ΔNp73 to the PDGFRB promoter, chromatin immunoprecipitation assays were done for SH-SY5Y and IMR-32 using p53, p73, ΔNp73, and p300 antibodies before and after addition of serum. The results showed that in IMR-32, ΔNp73 was bound constantly at all time points, whereas in SH-SY5Y, it was only bound in serum-starved cells and gradually decreased to around 20% of the initial level. In agreement with this, ΔNp73 was located in the nucleus of IMR-32, whereas in SH-SY5Y, it was found in the cytoplasm (result not shown). In contrast, the level of p73 binding was clearly increased after 4 hours to reach 2.5-fold at maximum after 8 hours of treatment in SH-SY5Y, whereas in IMR-32 the increase was small. p53 binding only slightly increased after 4 hours of treatment for SH-SY5Y, whereas for IMR-32, a clearly increased binding was seen at 8 and 24 hours. p300 remained bound to the promoter before and after serum addition, but with a gradual decrease (Fig. 2D; Supplementary Fig. S3). This suggests that the main difference between the two cell lines in PDGFRB promoter binding of p53 family members is a change in the ratio of ΔNp73 over total p73. In SH-SY5Y, the ratio of ΔNp73 over p73 was much smaller and minimal at 8 hours when total p73 binding increased and PDGFRB expression was repressed. In IMR-32, the increased binding of p73 after serum stimulation was small and the fraction of ΔNp73 was much larger. Moreover, the binding pattern observed in SH-SY5Y is closer to that seen in our previous studies of nontumor cell lines (11). The later increase of p53 binding in IMR-32 might explain the slight decrease in PDGFRB expression.

Cisplatin Represses PDGFRB Protein and mRNA Levels and Is Able to Induce p21 in Both SH-SY5Y and IMR-32 to Reduce Proliferation

We next examined the effects of the anticancer drug cisplatin to see whether the induced stabilization and modifications of p53 family members could decrease PDGFRB levels even in IMR-32. Following cisplatin treatment, PDGFRB protein levels decreased by about 60% at 24 to 48 hours in both cell lines. Moreover, both IMR-32 and SH-SY5Y cells treated for 12 hours with cisplatin showed increased levels of p53 protein and serine-15 phosphorylation (Fig. 3A; Supplementary Fig. S4). Following the same strategy as in Fig. 1, semiquantitative reverse transcription-PCR showed that PDGFRB mRNA displayed the same kinetics on cisplatin treatment, with a 40% decrease at 12 hours. This again showed the importance of transcriptional regulation as a feedback mechanism of PDGFRB

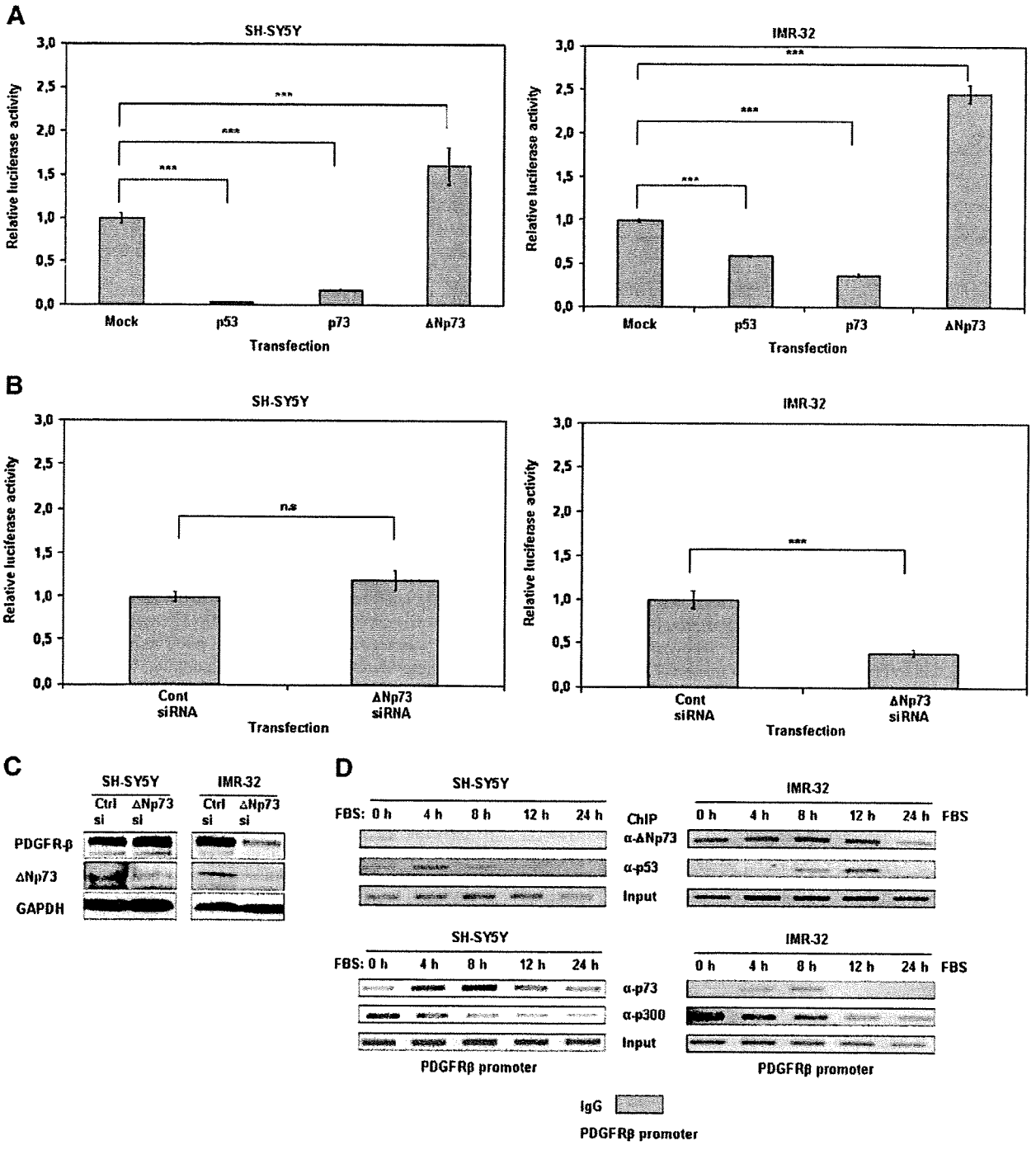

FIGURE 2. Differences between IMR-32 and SH-SY5Y in PDGFRB regulation by p53 family members. **A.** Cotransfection of ΔNp73 increases PDGFRB promoter activity, and p53 and p73 decrease promoter activity in both SH-SY5Y and IMR-32. SH-SY5Y and IMR-32 cells were transfected with PDGFRB promoter luciferase and LacZ constructs and cotransfected as indicated with a p53, p73, or ΔNp73 expression vector. Luciferase activity was measured 48 h later and values were adjusted to β-galactosidase. **B.** Cotransfection of ΔNp73 siRNA decreases PDGFRB promoter activity only in IMR-32. SH-SY5Y and IMR-32 cells were transfected with PDGFRB promoter luciferase and LacZ constructs and cotransfected with ΔNp73 siRNA as indicated and evaluated as above. **C.** Cotransfection of ΔNp73 siRNA represses PDGFRB protein expression only in IMR-32. SH-SY5Y and IMR-32 cells were transfected with scrambled siRNA or with ΔNp73 siRNA, as indicated, and cell lysates were immunoblotted with antibodies against PDGFRB and ΔNp73, with GAPDH as a standard. **D.** ΔNp73 binds strongly to the PDGFRB promoter, which is not displaced by p53 and p73 in response to serum stimulation in IMR-32, in contrast to almost no ΔNp73 binding in SH-SY5Y. SH-SY5Y and IMR-32 were serum starved for 48 h before being serum stimulated for the indicated time periods and chromatin immunoprecipitation assays were done. IgG was used as a negative control. Antibodies used are ΔNp73, p73 (E-4), p300, and p53 (DO-1) for IMR-32 or p53 (Ab-1) for SH-SY5Y.

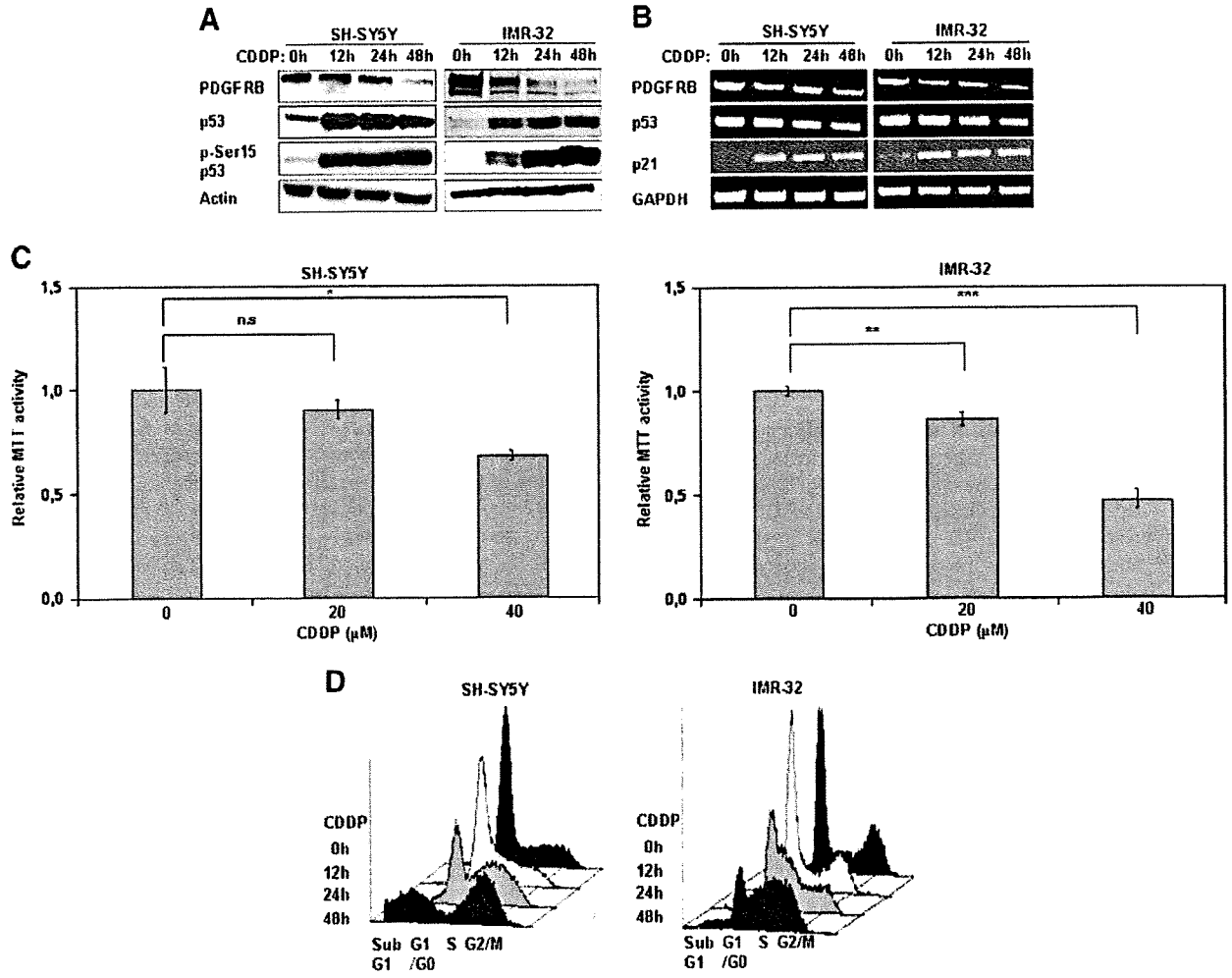

FIGURE 3. Cisplatin represses PDGFRB expression in both SH-SY5Y and IMR-32. Cells were treated with 20 μmol/L cisplatin for 0, 12, 24, and 48 h before harvest. **A.** Cisplatin represses PDGFRB protein expression and induces p53 serine-15 phosphorylation in both SH-SY5Y and IMR-32. Cell lysates were immunoblotted with antibodies against PDGFRB, p53, and p-Ser15-p53, with actin as a standard. **B.** Cisplatin represses PDGFRB mRNA expression and induces p21 in both SH-SY5Y and IMR-32. cDNA was reverse transcribed from cells treated with cisplatin, and the PCR products are shown for PDGFRB, p21, p53, and GAPDH. **C.** Cisplatin decreases proliferation of both SH-SY5Y and IMR-32. Cells were treated with 0, 20, or 40 μmol/L cisplatin for 24 h before MTT was added, and 4 h later, absorbance was measured at 570 nm. **D.** Cisplatin induces IMR-32 and SH-SY5Y cells to G_2-M arrest and increases the number of cells in sub-G_1-phase. Cells treated with cisplatin were run in a flow cytometer as described in the legend to Fig. 1D.

regulation. Furthermore, induction of the p53 target p21 mRNA was detected after cisplatin treatment in both cell lines, verifying that either p53 or p73 was functional in both cell lines (Fig. 3B; Supplementary Fig. S4).

Next, we compared the cellular responses of SH-SY5Y and IMR-32 with regard to proliferation and cell cycle phase distribution on cisplatin treatment to see whether IMR-32 had an increased resistance to cisplatin by its dysregulated PDGFRB expression, thus providing a prosurvival signal. MTT analysis showed that both cell lines decreased their metabolic activity, suggesting diminished proliferation in response to increasing cisplatin concentration (Fig. 3C). Fluorescence-activated cell sorting analysis revealed that cisplatin increased the sub-G_1 population in SH-SY5Y (from 2% to 21%), whereas cells that accumulated in G_2-M-phase decreased (from 11% to 5%). In contrast, the increase of the sub-G_1 cells was much smaller in IMR-32 (from 2% to 6%), which was almost refractory to cisplatin with regard to the number of cells in G_2-M-phase (from 14% to 16%; Fig. 3D; Table 2).

Cisplatin Represses PDGFRB Promoter Activity in Both SH-SY5Y and IMR-32, Displacing ΔNp73, and Recruits Binding of Histone Deacetylase 4 to the PDGFRB Promoter in IMR-32

The ability of cisplatin to affect PDGFRB promoter activity in each cell line was assessed using a luciferase assay of PDGFRB promoter activity. PDGFRB SacI/SacI was transfected and cotreated for 12, 24, or 48 hours with 0, 20, or 40 μmol/L cisplatin. For both cell lines, promoter activity decreased after 24 and 48 hours (Fig. 4A). In addition, in response to cisplatin treatment, ΔNp73α protein level increased in IMR-32 but remained constant in SH-SY5Y (Supplementary Fig. S5), in accordance with previous studies (19, 23), and was thus not the cause for the decreased PDGFRB expression.

Table 2. Cell Cycle Analysis of SH-SY5Y and IMR32 following CDDP Treatment

	Sub-G_1	G_1-G_0	S	G_2-M
0 h	2.0 ± 0.3	61.7 ± 1.4	22.8 ± 1.3	13.5 ± 2.1
12 h	2.9 ± 0.5	53.6 ± 3.0	32.3 ± 2.4	10.6 ± 2.1
24 h	3.8 ± 0.7	44.3 ± 10.2	41.1 ± 4.9	10.5 ± 4.0
48 h	20.9 ± 5.3	15.8 ± 4.3	54.6 ± 5.4	5.0 ± 0.5
	Sub-G_1	G_1-G_0	S	G_2-M
0 h	1.6 ± 1.1	54.6 ± 2.8	27.9 ± 2.7	16.4 ± 3.5
12 h	2.1 ± 0.4	53.5 ± 2.6	32.7 ± 2.8	11.6 ± 0.3
24 h	2.4 ± 0.6	40.4 ± 5.4	43.0 ± 4.8	13.6 ± 2.4
48 h	5.5 ± 1.1	19.6 ± 6.3	57.7 ± 6.6	15.5 ± 4.0

Because both cell lines thus far had displayed the same response to cisplatin for all experiments, only IMR-32 was investigated to see whether cotransfection of ΔNp73 siRNA would work synergistically with cisplatin to repress PDGFRB promoter activity. As seen in Fig. 4B, cotransfection of siRNA against ΔNp73 further decreased the promoter activity caused by cisplatin, indicating that ΔNp73 is removed from the PDGFRB promoter on cisplatin treatment.

To examine *in vivo* binding of p53, p73, and ΔNp73, as well as the binding of p300 and histone deacetylase (HDAC)-4 to the PDGFRB promoter, on cisplatin treatment, chromatin immunoprecipitation assays were done. The ΔNp73 binding to the PDGFRB promoter decreased by about 50% on cisplatin treatment. In contrast, the binding of p53 and p73 rather increased at 12 to 24 hours, and then decreased at 48 hours. Initially, p300 was bound to the promoter, but also decreased at 48 hours. HDAC4, on the other hand, was only found bound at 24 and 48 hours, indicating a repressed promoter at these time points (Fig. 4C; Supplementary Fig. S6).

Discussion

In normal cells, the binding of p53 family members to the PDGFRB promoter changes dynamically during serum-induced cell cycle progression. After serum stimulation, p73 and c-Myc are recruited to the PDGFRB promoter followed by HDAC1, reducing the promoter activity. This leads to a decrease in PDGFRB mRNA and protein levels, thereby providing a feedback mechanism (11). This study shows that the dysregulation of PDGFRB in IMR-32, as compared with SH-SY5Y, is associated with differences in the function of p53 family members, especially of ΔNp73. The fact that PDGFRB levels do not change in response to serum stimulation in IMR-32, whereas in the relatively differentiated neuroblastoma cell line SH-SY5Y, PDGFRB is regulated as in normal cells, underlines the importance of transcriptional regulation as a feedback mechanism.

Concerning the expression of p53 family members on serum addition, we expected to see differences between the two cell lines, as has been reported previously (24). However, we found a similar expression profile of p53 family members, including ΔNp73α, which acts as an activator of PDGFRB transcription in response to serum stimulation. Both p53 and p73 act as potent repressors on the PDGFRB promoter (9, 10), but we did not see any increase of p53 or p73α on serum treatment. Thus, the expression of p53 family members was not a factor responsible for the difference in the regulation of PDGFRB. Cellular context has previously been shown to be important for the different responses to p53 family members between cell lines (10, 25).

Another possible explanation for why PDGFRB expression is dysregulated in IMR-32 could be a possible dysfunction of the endogenous p53 or p73, perhaps as a result of mutation. However, no mutation of p53 or p73 has been reported in IMR-32. Interestingly, IMR-32, but not SH-SY5Y, responded strongly to silencing of ΔNp73 by repression of PDGFRB promoter activity and protein expression. A similar effect was seen when IMR-32 was transfected with ΔNp73-siRNA in addition to p53 and p73, which could be explained by the well-established dominant-negative effect of ΔNp73α in neuroblastoma. However, in SH-SY5Y, siRNA silencing of ΔNp73 did not yield any effect. This prompted us to investigate the promoter binding of the p53 family members. In IMR-32, ΔNp73 is constantly bound to the PDGFRB promoter at all time points following serum stimulation, whereas in SH-SY5Y, p73 binding markedly increases in parallel with the decreased binding of ΔNp73. This dynamic kinetics of the ratio of the bound ΔNp73/Np73 at different time points seems to correlate with the expression of the receptor. Thus, a larger fraction of ΔNp73 constitutively bound to the promoter in IMR-32 could explain the lack of downregulation on serum stimulation. The fact that p53 and p73 still bind the promoter in IMR-32 could be explained by the notion that ΔNp73 binds to DNA as an oligomer that could form heterooligomers with p53 and p73, inhibiting their activity (12, 20). Thus, increased binding of p53 and p73 to the PDGFRB promoter does not necessarily mean that the promoter is being repressed.

No observed significant effect of ΔNp73-siRNA expression on PDGFRB in SH-SY5Y concords with the weak binding of ΔNp73 to the PDGFB promoter (Fig. 2B). However, there is no clear explanation why the high expression of endogenous ΔNp73 does not result in similar binding as was seen for IMR-32. One possible explanation for this would be the post-translational modifications such as phosphorylation or acetylation that affect the capability of p53 family members to bind the promoter and execute their effects by recruitment of other proteins such as coactivators or repressors.

Because different stimuli can induce various modifications on p53 family proteins, we used the anticancer drug cisplatin. Cisplatin is known to activate p53 and p73 by kinase-mediated phosphorylation, thereby inducing p21 and proapoptotic proteins to result in cell cycle arrest and/or apoptosis. In fact, both neuroblastoma cell lines responded to cisplatin by downregulating PDGFRB at mRNA and protein levels, again showing the importance of the transcriptional regulation. Induction of p21 confirmed that either p53 or p73 was functioning in both cell lines. In agreement, cisplatin was able to repress PDGFRB promoter activity in both cell lines, although the decrease occurred slower in IMR-32. The small resistance to cisplatin may be due to ΔNp73 because the effect increased following the silencing of ΔNp73, leading to repression of PDGFRB promoter activity. Our chromatin immunoprecipitation experiments indeed showed that cisplatin initially decreased ΔNp73 binding to the PDGFRB promoter, whereas p53 and p73 binding increased.

The binding of p53 with HDAC4 was previously shown to be associated with the repressed PDGFRB promoter and its expression in normal fibroblasts (10). Thus, p53-stabilizing cytotoxic drugs can inhibit the high expression levels of PDGFRB maintained on serum stimulation in IMR-32.

It has previously been reported that Adriamycin-induced DNA damage recruits HDACs to NF-Y–dependent promoters, and that this recruitment depends on binding of p53 acetylated at the COOH-terminal lysines (26). This is concordant with what we have described here, although the PDGFRB promoter does not contain as many NF-Y binding sites as the G_2-M promoters (10). Thus, epigenetic modifications of p53 and/or p73 increase their binding affinities to NF-Y, enabling them to compete with ΔNp73 binding to NF-Y. It is likely that the modification on p53 and p73 on serum stimulation is not strong enough to repress the PDGFRB transcription in IMR-32.

It is well recognized that neuroblastoma consists of highly heterogeneous tumor subtypes with marked differences in phenotypes, tumor localization, and invasiveness, which are manifested by varying therapy responses and prognosis, constituting a major problem in clinics. Therefore, identification of the mechanism responsible for their diversity could help in improving therapeutic strategy. Our findings indicate that neuroblastoma with overexpression of ΔNp73α might not respond by downregulating PDGFRB expression in a microenvironment containing PDGF ligands, thereby providing a constitutive stimulus for cell proliferation. It is necessary to examine primary neuroblastoma cells to conclude if this is the case *in vivo*. It has been shown that ΔNp73 status correlates with prognosis of patients with different tumors and responsiveness to cytostatic drugs (13, 27).

It has been shown that the affinities of p53 to different promoters are associated with its epigenetic modification, affecting its functional outcome (i.e., cell cycle arrest or apoptosis in cells; ref. 28). If this is the case, the epigenetic modification status of ΔNp73 when binding to different promoters should

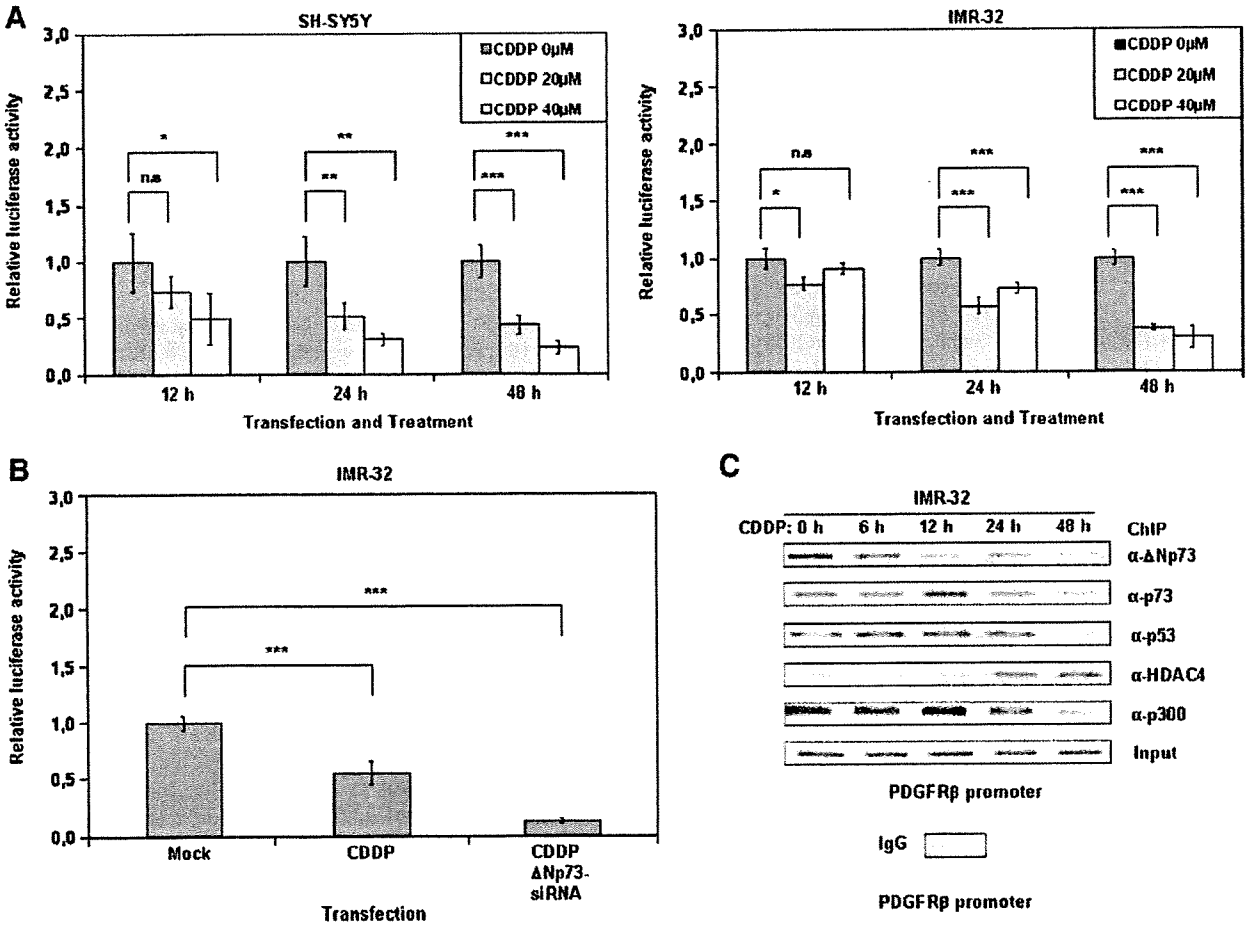

FIGURE 4. Cisplatin displaces ΔNp73 from the PDGFRB promoter to repress its activity. **A.** Cisplatin decreases PDGFRB promoter activity in both SH-SY5Y and IMR-32. SH-SY5Y and IMR-32 cells were transfected with PDGFRB promoter luciferase and LacZ constructs and treated with 0, 20, or 40 μmol/L cisplatin for 12, 24, and 48 h. Luciferase activity was measured as described in the legend to Fig. 2A. **B.** Cotransfection of ΔNp73 siRNA synergistically represses PDGFRB activity with cisplatin treatment in IMR-32. Cells were transfected with PDGFRB promoter luciferase and LacZ constructs and cotransfected with siRNA and 20 μmol/L cisplatin as indicated. Luciferase activity was measured 48 h later and values were adjusted to β-galactosidase and protein concentration. **C.** Cisplatin displaces ΔNp73 and recruits binding of HDAC4 to the PDGFRB promoter to repress its activity in IMR-32. Cells were treated with 20 μmol/L cisplatin for 0, 6, 12, 24, and 48 h, and chromatin immunoprecipitation assays were done. PCR products for the PDGFRB promoter are shown. An aliquot for each lysate was used as input for the PCR with the antibodies indicated on the right.

be determined by its competition with modified p53, which then affects its cellular consequences. In this context, it is also important to investigate whether cisplatin could dissociate ΔNp73 from genes other than the *PDGFRB* gene that are controlled by the p53 family of tumor suppressors.

In summary, results in this report implicate ΔNp73 binding to the PDGFRB promoter as a determinant of dysregulated PDGFRB expression and as a possible factor that stimulates autocrine or paracrine PDGF signaling.

Materials and Methods

Cell Lines, Cultures, and Drugs

Neuroblastoma cell lines SH-SY5Y and IMR-32 were maintained in DMEM and RPMI 1640, respectively, both supplemented with heat-inactivated 10% fetal bovine serum (FBS), 100 units/mL penicillin, and 60 μg/mL streptomycin. Cells were cultured in a humidified 5% CO_2 atmosphere at 37°C. For serum stimulation studies, cells were serum starved for 48 h with 0.5% FBS for SH-SY5Y or with 0.1% FBS for IMR-32. Thereafter, 10% FBS was added to the media and cells were harvested after 0, 4, 8, 12, 24, and 48 h. For cisplatin experiments, cells were incubated with 20 μmol/L cisplatin, unless otherwise stated, for the indicated time periods.

Plasmid Constructs and Antibodies

For luciferase reporter assays, the PDGFRB promoter cloned into the luciferase expression vector pGL3 (Promega) was used. p53, p73α, and ΔNp73α were expressed in pcDNA3 vectors. The antibodies used were PDGFRB (958), p-PDGFRB (1021), p53 (DO1), p73 (H-79), p73 (E-4), p300 (N-15), and HDAC4 (H-92), all from Santa Cruz; HDAC1 (H-3284) and β-actin (AC-40) from Sigma; p53 (Ab-1) from Calbiochem; and p-Akt (T308) from R&D Systems.

Luciferase Assays

SH-SY5Y and IMR-32 cells were transfected with 0.25 μg of reporter plasmid, 0.25 μg of β-galactosidase expression plasmid, and 0.5 μg of expression plasmids or mock DNA vector. Transfection of neuroblastoma cell lines was facilitated by the use of the magnetofectin transfection system (Oz Bioscience). To each microgram of DNA, 1 μL of Combimag cationic magnetic beads was added. The DNA-bead complexes were diluted in serum-free medium and mixed with Fugene6 transfection reagent for SH-SY5Y cells or with Lipofectamine 2000 for IMR-32 cells, and then incubated according to the manufacturers' instructions. Luciferase activity was adjusted to β-galactosidase activity, and for luciferase assays in studying the effect of cisplatin, it was adjusted to protein concentration as well. Measured values are displayed as means with SDs ($n = 3$). ANOVA was used to test significant differences. Between-group significance was determined with Scheffé's post hoc test. $P < 0.05$ was considered statistically significant. * indicates $P < 0.05$, ** indicates $P < 0.01$, and *** indicates $P < 0.001$.

Small Interfering RNA

siRNA against ΔNp73 (20 nmol/L; Qiagen) was microporated into IMR-32 and SH-SY5Y using a microporator (Digital Bio) according to the manufacturer's instructions.

Chromatin Immunoprecipitation

SH-SY5Y and IMR-32 cells were seeded in 10-cm dishes and cross-linked and harvested when cells were 80% confluent. DNA and protein were cross-linked with 1% formaldehyde for 15 min at 37°C. Cell lysis, sonication, immunoprecipitation, and PCR were done as described (11). For the proximal human PDGFB promoter, primers were 5′-AGCATCCCCTCACATCCTGAGCGA-3′ and 5′-CAGGAGCTCACACCACTATGGGCT-3′. Series of dilutions of prepared DNA were used and amplified for an optimal number of cycles.

Reverse transcription-PCR

SH-SY5Y and IMR-32 cells were seeded in 12-cm dishes at a density of 5×10^4 per dish. RNA extracted with RNeasy Minikit (Qiagen) was extracted essentially as described (29). Total RNA (1-3 μg) was subsequently transcribed into cDNA with random primers and SuperScriptIII reverse transcriptase (Invitrogen) according to the manufacturer's protocol. PCR was carried out by using Taq polymerase (Invitrogen) using one-tenth of the cDNA. Primers were designed as follows, 5′-TCAACGTCTCTGTGAACGCAGTGC-3′ and 5′-GCCCAGGGTGCGGTTGTCTTTGAA-3 for PDGFRB; 5′-AAGATGACCCAGATCATGTTTGAG-3′ and 5′-AGGAGGAGCAATGATCTTGATCTT-3 for α-actin; ΔNp73, p73, p53, p21, and glyceraldehyde-3-phosphate dehydrogenase (GAPDH) primers were designed as previously described (30). PCR products were analyzed on a 2.0% Tris-acetate-EDTA-agarose gel with ethidium bromide and scanned in a FLA2000 (Fuji).

Immunoblotting

SH-SY5Y and IMR-32 cells were seeded in six-well plates at 1×10^5 per well. Cells were lysed in lysis buffer [25 mmol/L Tris-HCl (pH 7.5), 137 mmol/L NaCl, 2.7 mmol/L KCl, 1% Triton X-100, and 1 mmol/L phenylmethylsulfonyl fluoride] and sonicated 12 times with 0.5-s pulses at 80% power using a VibraCell (Chemical instruments AB). Proteins were separated on an 8% SDS-PAGE and transferred onto a Hybond-C extra polyvinylidene difluoride membrane (Amersham Biosciences). Membranes were blocked overnight in 5% skim milk at 4°C. Primary antibodies were diluted in 5% skim milk and incubated for 1 h at room temperature, followed by incubation for 45 min with secondary antibody. Membranes were developed using the ECL Advance system according to the manufacturer's protocol (GE Healthcare) and scanned using LAS-1000 Plus (Fujifilm).

Flow Cytometry

SH-SY5Y and IMR-32 cells were seeded in 10-cm dishes and harvested at 50% to 80% confluency. Cells were trypsinized and centrifuged at 1,200 rpm for 5 min. Cells were washed twice with PBS before resuspending the cell pellet in 200 μL of PBS. Thereafter, cells were fixed for 30 min by addition of ice-cold 70% ethanol. Cells were centrifuged and washed in PBS before being stained with propidium iodine (40 μg/mL) in the presence of RNase A (50 μg/mL) for 30 min at 37°C. Cells were washed and cell aggregates were removed using a mesh. Cell cycle analysis was done on a FACSCalibur (Becton Dickinson) using the CellQuest software. FL2-H, FL2-A, and FL2-W were detected. Using FL2-H against

FL2-W dot plot, aggregates were gated out, with at least 10,000 events gated and analyzed.

MTT Assay

SH-SY5Y and IMR-32 cells were seeded in 96-well plates at 0.3×10^5 per well. After treatment with drugs, cell proliferation was measured by adding 20 μL of 5 mg/mL MTT. After 4 h at 37°C, medium was removed and formazan crystals were dissolved in DMSO. Absorbance was measured at 570 nm.

Disclosure of Potential Conflicts of Interest

No potential conflicts of interest were disclosed.

References

1. Heldin CH, Westermark B. Mechanism of action and *in vivo* role of platelet-derived growth factor. Physiol Rev 1999;79:1283–316.

2. Liu P, Ying Y, Ko YG, Anderson RG. Localization of platelet-derived growth factor-stimulated phosphorylation cascade to caveolae. J Biol Chem 1996;271: 10299–303.

3. Sorkin A, Westermark B, Heldin CH, Claesson-Welsh L. Effect of receptor kinase inactivation on the rate of internalization and degradation of PDGF and the PDGF β-receptor. J Cell Biol 1991;112:469–78.

4. Mori S, Heldin CH, Claesson-Welsh L. Ligand-induced polyubiquitination of the platelet-derived growth factor β-receptor. J Biol Chem 1992;267:6429–34.

5. Oster SK, Marhin WW, Asker C, et al. Myc is an essential negative regulator of platelet-derived growth factor β receptor expression. Mol Cell Biol 2000;20: 6768–78.

6. Izumi H, Molander C, Penn LZ, Ishisaki A, Kohno K, Funa K. Mechanism for the transcriptional repression by c-Myc on PDGF β-receptor. J Cell Sci 2001;114: 1533–44.

7. Guha A, Dashner K, Black PM, Wagner JA, Stiles CD. Expression of PDGF and PDGF receptors in human astrocytoma operation specimens supports the existence of an autocrine loop. Int J Cancer 1995;60:168–73.

8. Hermanson M, Funa K, Hartman M, et al. Platelet-derived growth factor and its receptors in human glioma tissue: expression of messenger RNA and protein suggests the presence of autocrine and paracrine loops. Cancer Res 1992;52:3213–9.

9. Hackzell A, Uramoto H, Izumi H, Kohno K, Funa K. p73 independent of c-Myc represses transcription of platelet-derived growth factor β-receptor through interaction with NF-Y. J Biol Chem 2002;277:39769–76.

10. Yang W, Wetterskog D, Matsumoto Y, Funa K. Kinetics of repression by modified p53 on the PDGF B-receptor promoter. Int J Cancer 2008;123:2020–30.

11. Uramoto H, Wetterskog D, Hackzell A, Matsumoto Y, Funa K. p73 competes with co-activators and recruits histone deacetylase to NF-Y in the repression of PDGF β-receptor. J Cell Sci 2004;117:5323–31.

12. Zaika AI, Slade N, Erster SH, et al. ΔNp73, a dominant-negative inhibitor of wild-type p53 and TAp73, is up-regulated in human tumors. J Exp Med 2002; 196:765–80.

13. Casciano I, Mazzocco K, Boni L, et al. Expression of ΔNp73 is a molecular marker for adverse outcome in neuroblastoma patients. Cell Death Differ 2002;9: 246–51.

14. Concin N, Becker K, Slade N, et al. Transdominant ΔTAp73 isoforms are frequently up-regulated in ovarian cancer. Evidence for their role as epigenetic p53 inhibitors *in vivo*. Cancer Res 2004;64:2449–60.

15. Hollstein M, Sidransky D, Vogelstein B, Harris CC. p53 mutations in human cancers. Science (New York, NY) 1991;253:49–53.

16. White PS, Maris JM, Beltinger C, et al. A region of consistent deletion in neuroblastoma maps within human chromosome 1p36.2–36.3. Proc Natl Acad Sci U S A 1995;92:5520–4.

17. Kaghad M, Bonnet H, Yang A, et al. Monoallelically expressed gene related to p53 at 1p36, a region frequently deleted in neuroblastoma and other human cancers. Cell 1997;90:809–19.

18. Grob TJ, Novak U, Maisse C, et al. Human δNp73 regulates a dominant negative feedback loop for TAp73 and p53. Cell Death Differ 2001;8: 1213–23.

19. Nakagawa T, Takahashi M, Ozaki T, et al. Autoinhibitory regulation of p73 by ΔNp73 to modulate cell survival and death through a p73-specific target element within the ΔNp73 promoter. Mol Cell Biol 2002;22:2575–85.

20. Stiewe T, Theseling CC, Putzer BM. Transactivation-deficient ΔTA-p73 inhibits p53 by direct competition for DNA binding: implications for tumorigenesis. J Biol Chem 2002;277:14177–85.

21. Fritsche M, Haessler C, Brandner G. Induction of nuclear accumulation of the tumor-suppressor protein p53 by DNA-damaging agents. Oncogene 1993;8: 307–18.

22. Gong JG, Costanzo A, Yang HQ, et al. The tyrosine kinase c-Abl regulates p73 in apoptotic response to cisplatin-induced DNA damage. Nature 1999;399: 806–9.

23. Million K, Horvilleur E, Goldschneider D, et al. Differential regulation of p73 variants in response to cisplatin treatment in SH-SY5Y neuroblastoma cells. Int J Oncol 2006;29:147–54.

24. Goldschneider D, Million K, Meiller A, et al. The neurogene BTG2TIS21/PC3 is transactivated by ΔNp73α via p53 specifically in neuroblastoma cells. J Cell Sci 2005;118:1245–53.

25. Uramoto H, Hackzell A, Wetterskog D, Ballagi A, Izumi H, Funa K. pRb, Myc and p53 are critically involved in SV40 large T antigen repression of PDGF β-receptor transcription. J Cell Sci 2004;117:3855–65.

26. Basile V, Mantovani R, Imbriano C. DNA damage promotes histone deacetylase 4 nuclear localization and repression of G_2/M promoters, via p53 C-terminal lysines. J Biol Chem 2006;281:2347–57.

27. Uramoto H, Sugio K, Oyama T, et al. Expression of ΔNp73 predicts poor prognosis in lung cancer. Clin Cancer Res 2004;10:6905–11.

28. Knights CD, Catania J, Di Giovanni S, et al. Distinct p53 acetylation cassettes differentially influence gene-expression patterns and cell fate. J Cell Biol 2006;173:533–44.

29. Chomczynski P, Sacchi N. Single-step method of RNA isolation by acid guanidinium thiocyanate-phenol-chloroform extraction. Anal Biochem 1987;162: 156–9.

30. Hayashi S, Ozaki T, Yoshida K, et al. p73 and MDM2 confer the resistance of epidermoid carcinoma to cisplatin by blocking p53. Biochem Biophys Res Commun 2006;347:60–6.

Imaging, Diagnosis, Prognosis

Clinical Cancer Research

Accurate Outcome Prediction in Neuroblastoma across Independent Data Sets Using a Multigene Signature

Katleen De Preter[1], Joëlle Vermeulen[1], Benedikt Brors[2], Olivier Delattre[4], Angelika Eggert[5], Matthias Fischer[6], Isabelle Janoueix-Lerosey[4], Cinzia Lavarino[7], John M. Maris[8], Jaume Mora[7], Akira Nakagawara[9], André Oberthuer[6], Miki Ohira[9], Gudrun Schleiermacher[4], Alexander Schramm[5], Johannes H. Schulte[5], Qun Wang[8], Frank Westermann[3], Frank Speleman[1], and Jo Vandesompele[1]

Abstract

Purpose: Reliable prognostic stratification remains a challenge for cancer patients, especially for diseases with variable clinical course such as neuroblastoma. Although numerous studies have shown that outcome might be predicted using gene expression signatures, independent cross-platform validation is often lacking.

Experimental Design: Using eight independent studies comprising 933 neuroblastoma patients, a prognostic gene expression classifier was developed, trained, tested, and validated. The classifier was established based on reanalysis of four published studies with updated clinical information, reannotation of the probe sequences, common risk definition for training cases, and a single method for gene selection (prediction analysis of microarray) and classification (correlation analysis).

Results: Based on 250 training samples from four published microarray data sets, a correlation signature was built using 42 robust prognostic genes. The resulting classifier was validated on 351 patients from four independent and unpublished data sets and on 129 remaining test samples from the published studies. Patients with divergent outcome in the total cohort, as well as in the different risk groups, were accurately classified (log-rank $P < 0.001$ for overall and progression-free survival in the four independent data sets). Moreover, the 42-gene classifier was shown to be an independent predictor for survival (odds ratio, >5).

Conclusion: The strength of this 42-gene classifier is its small number of genes and its cross-platform validity in which it outperforms other published prognostic signatures. The robustness and accuracy of the classifier enables prospective assessment of neuroblastoma patient outcome. Most importantly, this gene selection procedure might be an example for development and validation of robust gene expression signatures in other cancer entities. *Clin Cancer Res; 16(5); 1532–41. ©2010 AACR.*

One of the main challenges in clinical cancer research remains accurate prediction of outcome, enabling better choice of risk-related therapy. This is particularly true for neuroblastoma, a pediatric tumor of the sympathetic nervous system, which is characterized by a remarkably heterogeneous clinical course. Tumors that are found in infants frequently regress spontaneously or show differentiation features on treatment, whereas tumors diagnosed in children >1 year of age often metastasize, causing accelerated cancer-related death despite intensive therapies. Accordingly, different therapeutic schemes exist ranging from watch-and-see approaches to multimodal therapies. Four major risk stratification systems are currently being used in various parts of the world (Europe, United States, Japan, and Germany) based on a combination of clinicopathologic and genetic parameters, such as age at diagnosis, tumor stage, *MYCN* gene status, histopathologic classification, ploidy, and chromosome 1p and 11q status (1–8). Clinical experience within these systems indicates that the stratification is useful, but misclassifications occur, resulting in overtreatment or undertreatment. Identification of more specific and sensitive markers for response to therapy and outcome prediction is clearly required and is expected to result in better choice of risk-related therapy.

As differences in outcome are considered to reflect underlying genetic and biological characteristics that have

Authors' Affiliations: [1]Center for Medical Genetics, Ghent University, Ghent University Hospital, Ghent, Belgium; Departments of [2]Theoretical Bioinformatics and [3]Tumour Genetics, German Cancer Research Center, Heidelberg, Germany; [4]Institut National de la Sante et de la Recherche Medicale U830, Institut Curie, Paris, France; [5]Division of Hematology and Oncology, University Children's Hospital Essen, Essen, Germany; [6]Children's Hospital of Cologne, Department of Pediatric Oncology, Cologne, Germany; [7]Developmental Tumor Biology Laboratory, Hospital Sant Joan de Déu, Barcelona, Spain; [8]Division of Oncology, Children's Hospital of Philadelphia, University of Pennsylvania School of Medicine, Philadelphia, Pennsylvania; and [9]Division of Biochemistry, Chiba Cancer Center Research Institute, Chiba, Japan

Corresponding Author: Jo Vandesompele, Center for Medical Genetics, Ghent University Hospital, Medical Research Building, 2nd Floor, Room 120.055, De Pintelaan 185, B-9000 Ghent, Belgium. Phone: 32-9-332-5187; Fax: 32-9-332-6549; E-mail: Joke.Vandesompele@UGent.be.

doi: 10.1158/1078-0432.CCR-09-2607